Polyphase tectonic, thermal and burial history of the Vocontian basin revealed by U-Pb calcite dating

Louise Boschetti[1], Malou Pelletier[1], Frédéric Mouthereau[1,2], Sté~~e~~phane Schwartz[3], Yann Rolland[3,4], Guilhem Hoareau[5], Thierry Dumont[3], Dorian Bienveignant[3], Abdeltif Lahfid[6]

1. Géosciences Environnement Toulouse, Université de Toulouse Paul Sabatier, CNRS, IRD, 14 av. Edouard Belin, 31400 Toulouse, France
2. Institut Universitaire de France, F-75005 Paris, France
3. ISTerre, Université Grenoble Alpes, USMB, CNRS, IRD, UGE, 38000 Grenoble, France.
4. EDYTEM, Université Savoie Mont Blanc, CNRS, UMR 5204, Le Bourget du Lac, France.
5. Université de Pau et des Pays de l'Adour, E2S UPPA, CNRS, LFCR, UMR5150, Pau, France.
6. BRGM, B.P. 6009, 45060 Orléans Cedex, France

Corresponding author: louise.boschetti@univ-tlse3.fr

Abstract

The Vocontian Basin in southeastern France records a long-lived history of subsidence and polyphase deformation at the junction of Alpine and Pyrenean orogenic systems. This study aims to reconstruct~~ed~~ the ~~geodynamical~~ tectonic, ~~and thermal~~burial and thermal evolution of this basin, based on new U–Pb dating of calcite from veins and faults combined with new RSCM thermometry and stratigraphy-based burial models. Three main generations of calcite~~s~~ are ~~dated~~identified: (1) the Late Cretaceous to Paleocene ~~dates~~ period related to the Pyrenean-Provençal convergence (~84–50 Ma); (2) the Oligocene period ~~dates~~ linked to the extension of the West European Rift ~~extension~~ (~30–24 Ma); and (3) the Miocene ~~dates~~ period, ascribed to strike-slip and compression associated with the Alpine collision (~12–7 Ma). No older ages related to the Jurassic and Early Cretaceous rifting phase~~s~~ are obtained, despite ~~specific~~ targeted sampling near normal faults~~ing,~~ suggesting ~~limited~~ focused syn-rift fluid circulation or ~~subsequent~~ dissolution of early calcite mineralization during subsequent tectonic events. RSCM data highlight a pronounced ~~E~~east–~~W~~ west thermal gradient.~~,~~ ~~with p~~Peak temperatures are below 100°C in the west and exceed~~ing~~ 250°C in the eastern basin, ~~. This is, consistent with a~~

more significant reflecting greater crustal thinning and/or salt diapirism in the eastern part of the Vocontian Basin inwith the overlapping -relation to the superimposed Jurassic and Cretaceous rifting phases. These results emphasize the large-scalesignificant impact of the opening of the West European Rift in south-easternSE France. They further -and highlight the potential discrepancymismatch underscore the possible mismatch between the large-scale tectonic processess and the tectonic history inferred from calcite U–Pb dating, which . This method , which is sensible sensitive to the presence of fluids and the physical conditions necessaryrequired for their preservations.

1. Introduction

Sedimentary basins located in the external part of orogenic belts can offer provide critical insights into the polyphase and complex evolution of tectonic plate boundaries. The Vocontian Basin is located at the front of the southern Alpine belt in southeastern France is currently positioned at the front of the southern Alpine belt, to the north of Provence (Fig. 1, 2A). This basin region recorded a succession of tectonic events spanning from the Late Mesozoic Cretaceous to the Cenozoic (Roure et al., 1992; Homberg et al., 2013; Mouthereau et al., 2021). They are , (Fig. 1). They are attributed to Mesozoic . These different tectonic events have been attributed to the Mesozoic rifting associated with therifting opening ofin the Alpine Tethys and the Atlantic Ocean-Pyrenean riftsystems, Cenozoic inversion of the rifted margins during the development of the Pyreneanes-Provence collision, and the Eocene-Oligocene to Miocene extension associated with the opening of the West European Rift and the opening of the Gulf of Lion -(e.g., Stämpfli, 1993; Homberg et al., 2013; Bestani et al., 2016; Espurt et al., 2019; Célini et al., 2023).

Some dDetails of the tectonic evolution of the Vocontian Bbasin specifically, positioned at the intersection between the Europe-Iberia and Europe-Adria plate plate boundaries, are however debated. There has been aA long-standing debate persists abouton on whether the Mid-Cretaceous Vocontian Basin , north of Provence, is part of a continuous rift system linking between the Valaisan bBasin and the /Alpine Tethys in the east andto the Pyrenean Bbasin and /Atlantic Ocean Ocean in the west (Trümpy, 1988; Stämpfli, 1993; Stämpfli and Borel, 2002; Turco et al., 2012), or if it. In contrast, other studies suggest that the Vocontian Basin, while belongsging to the broader Pyrenean/Atlantic rift system., remained structurally disconnected from other Pyrenean and Provençal riftwithIn the latter case, Provence would be a small emerged continental domain that is structurally disconnected from the Pyrenean and Provençal rifts segments (Debelmas, 2001; Manatschal and Muntener, 2009; Angrand and Mouthereau, 2021; Célini et al., 2023; Boschetti et al., 2025a,b). In the latter hypothesis, Provence forms a rather small emerged continental domain between two Cretaceous rift segments.

The analyses of Raman Spectroscopy of Carbonaceous Material (RSCM) temperatures from the Digne Nappe, in the eastern part of the Vocontian basin (Fig. 2A), supports a tectonic model in which the Vocontian basin resulted from two superimposed phases of crustal thinning. The first one is dated to the Upper Jurassic and coincides with the Alpine Tethys opening. The second phase, characterised by temperatures in the basin exceeding 300°C, is believed to have occurred during the Lower Cretaceous period, when the Pyrenean rifting led to continental breakup in the Valaisan domain (Célini et al., 2023).

Despite the presence of the well-established structural and sedimentary constraints evidence on showof the tectonic evolution of the basin, including clear evidence for mid-Cretaceous syn-depositional normal faulting in the basin in the mid-Cretaceous (e.g., Homberg et al., 2013), brittle deformation lacks precise geochronological constraints data on the timing of this rifting and subsequent inversion are lacking. Establishing this chronology is critical, as the Cretaceous extension often overlaps with the onset of Pyrenean compression (Fig. 2B) and could also be linked to diapirism (Bilau et al., 2023b). Resolving this question is criticalimportant because, as the timing of the end of Cretaceous extension often overlaps coincides with the onset of Pyrenean compression (Fig. 2B) also be related to(Bilau et al., 2023b). Furthermore, itIt is also is unclear whether this part of the Alpine foreland was tectonically affected by experienced the Eo-Oligocene same extension associated as the West European Rift extension , as seen in nearby in the Valence and Manosque basins (e.g., Ford and Lickorish, 2004), or with the opening of the West Mediterranean well identified in the thermal record of the Maures-Esterel massif, a few tens of kilometers to the south ((Fig. 2B) (Boschetti et al., 2023; 2025a,b). SuchThese Cenozoic thinning events may have impacted the thermal evolution of the Vocontian Basin and be confused with Mid-Cretaceous extension or Alpine thickening (Fig. 2B) (e.g., Célini et al., 2023). In addition, two Nnorth-Ssouth compressional events dated to Eocene and late Miocene are recognized in the fault pattern of Provence (Bergerat et al., 1987; Lacombe and Jolivet, 2005). . The role of all these major tectonic phases in the brittle deformation history and in the related thermal regime remains unclear as, the most recent studies in the basin have not yet successfully isolated the effects of each been able to discretise the influences of each of these geodynamic events within the basin and their impact. In particular, the temperatures reconstructed based on reconstructions based on analyseis of Raman Spectroscopy of Carbonaceous Material (RSCM) support two alternative tectonic scenarios. (i) Either the tTemperatures from the Digne Nappe are interpreted as resultingreflect fromcrustal thickening below the propagating Alpine nappe stack (Balansa et al., 2023). An alternativeAlternatively, a scenarimodelo supports a tectonic model ofinvolving two superimposed phases of crustal thinning in the Vocontian basin has been proposed (Célini et al., 2023; Fig. 2BA). The first phase, is tied up toin the Upper Jurassic, and coincides with the Alpine Tethys opening, while the . The second phase, characterised by temperatures exceeding 300°C duringin the Lower Cretaceous, is associated with Pyrenean rifting and Valaisan opening (Célini et al., 2023). Therefore, large-scaleBasin-scale geochronological and thermal analyses tectonic implications of the thermal evolution of Vocontian basin need to be confirmed by a combined geochronological and thermal approach at the scale of the basinare needed to validate this tectonic intepretations.

This study addresses these questions through usingby an approach combining basin-scale U-Pb dating of calcite in faults and veins, -which origins are constrained constrained by paleostress inversions, complemented with new RSCM thermochronologytemperatures and anand the analysis of the analysis of the burial history analysis of the Vocontian basinBasin. Our. We aim is to establish a robust chronological framework for the Vocontian basin in the context of the , related to the geodynamics of SEsouth-east France, and to clarifying the interactions betweensuccessionsequence and extent of the different successive tectonic systemsphases that developed in SE France by establishing a robust chronological framework. Our findingTheses constraints have significant implications forimprove our understanding of polyphase deformation at the Europe-Iberia-Adria plate boundary.

The analyses of Raman Spectroscopy of Carbonaceous Material (RSCM) temperatures from the Digne Nappe, supports a tectonic model of two superimposed phases of crustal thinning in the Vocontian basin (Fig. 2A). The first phase is dated to the Upper Jurassic and coincides with the Alpine Tethys opening. The second phase, characterised by temperatures exceeding 300°C during the Lower Cretaceous, is associated with Pyrenean rifting and Valaisan opening (Célini et al., 2023). To gain insights on the large-scale tectonic implications of the thermal evolution of Vocontian basin, temperature constraints have been obtained in eastern part of the Vocontian Basin that was inverted during the Alpine collision, and transported in the Digne Nappe. Large-scale tectonic implications of the thermal evolution of Vocontian basin did to be confirmed in the Vocontian Basin

2. Geological setting

Positioned at the front of the Western Alps, the Vocontian Basin ~~is~~ forms part of the Southern Subalpine belt, which developed ~~produced~~ through ~~by~~ the interactions between the Pyrenean-Provençal belt to the south and the Alpine belt to the east (Philippe et al., 1998; Balansa et al., 2022; Célini et al., 2024; Fig. 1). It includes the Diois-Baronnies region, and ~~it~~ is bordered by the Rhône Valley and the French Massif Central basement to the west, the External Crystalline Massif of Pelvoux to the east, the Vercors Massif to the north, and the Provençal Platform to the south (Figs. 1, 2A).

The Vocontian Basin ~~is filled by with a succession approximately 2,600 m thick succession of~~contains a thick ~~mostly~~ Mesozoic sedimentary succession, ~~deposits, along its margins~~ reaching ~~a thickness of~~ up to 7,000 m in ~~its the~~its center and 2,600 m along its margins (Fig. 2B).

The base of the folded stratigraphic sequence ~~is made of~~comprises U~~u~~pper Triassic evaporites, which have ~~led~~ resulted ~~to~~ in the ~~development~~ formation of salt diapirs ~~that piercing pierce the sedimentary cover~~ (e.g. Suzette and~~,~~ Propiac diapirs) that pierce the overlying sedimentary cover ~~, or as well as~~and locally controll~~ing~~ ~~certain features of the basin including such as variations in~~ thickness variations ~~variations~~ (Fig. 3A) (Célini, 2020 and references therein).

~~The subsidence at the origin of that formed the basin~~Basin subsidence ~~initiated~~ began with the opening of the Alpine Tethys ~~to the east~~ during the Early to Middle Jurassic (e. g. Lemoine et al., 1986). This period is marked by the deposition of alternating shallow marine limestones and marls, followed by progressive deepening that culminated with ~~marine environments culminating with~~ the deposition of organic-rich black shales of the "Terres Noires" formation during the Bathonian–Oxfordian (Fig. 2). In the Late Jurassic, the basin underwent NNE–SSW-directed extension, ~~as~~ recorded by syn-sedimentary NNW–SSE-trending normal faults (Homberg et al., 2013). This extensional regime, ~~consistent~~ linked to ~~with~~ the propagation of the Alpine Tethys, led to the deposition of fine-grained bioclastic Tithonian l~~L~~imestones, which ~~form~~ serves as a distinctive morphostructural marker and reflect slower subsidence (Remane, 1970; Joseph et al., 1988). The subsidence continued through~~out~~ the Early Cretaceous (Valanginian-Aptian)~~ period~~, with the ~~during which~~deposition of alternating layers of marls and limestones ~~were deposited~~that define ~~, shaping~~ the deeper marine "Vocontian facies", contrasting with ~~. These deeper marine deposits contrast with the~~ shallow-water carbonates of the Vercors and Provence platforms~~ to the north~~, known as the "Urgonian facies" (Fig. 2A).

A major tectonic shift ~~in the tectonic regime~~ occurred during the Aptian–Albian~~ period~~, which ~~was marked~~ characterised by increased subsidence and the deposition of thick marly sequences ("Blue Marls"; Debrand-Passard et al., 1988) (Fig. 2B). This phase is associated with the development of E–W-trending normal faults, suggesting a reorientation of the extensional stress field from NNE–SSW (Late Jurassic) to WNW–ESE (Homberg et al., 2013). This shift ~~is interpreted to~~likely reflect-s plate tectonic reorganization, linked to the onset of Europe–Iberia divergence (Bay of Biscay opening) and the closure of the Alpine Tethys through Europe-Adria convergence (Lemoine et al., 1987; Stämpfli, 1993).

During the Late Cretaceous, sandstones ~~were~~ deposition~~ed~~ dominated in the east of the basin, while limestones prevailed in the west ~~whereas limestones predominated in the east of the basin~~ (Fig. 2). In the north-eastern part of the basin, ~~At~~ at the current location of the Dévoluy massif, ~~in the north-eastern part of the basin,~~ a stratigraphic hiatus ~~of~~ spanning the Turonian, Coniacian to the Santonian (Fig. 3B) is documented, regionally referred to as the Turonian unconformity (e. g. Flandrin, 1966). ~~It is marked~~ This interval is characterized by the argillaceous to sublithographic ~~limestones of the~~ lower Cretaceous limestones and E-W--trending folds, which ~~are~~ lie in direct contact, below an erosional surface, with ~~bioclastic and terrigenous deposits of the~~ Campanian-Maastrichtian bioclastic and terrigenous deposits ~~-~~(Fig. 2-3B; Gidon et al., 1970; Arnaud et al., 1974). ~~In the entire~~Across the Vocontian basin, the main stratigraphic hiatus corresponds to the Paleocene-Early Eocene (Fig. 2B). This late Cretaceous~~- to -~~Paleocene event ~~is~~ coincides ~~coeval~~ with the onset of Iberia-Europe convergence, marking the initial stages of the Pyrenean-Provençal orogeny ~~from ~84 Ma~~ (~84 Ma; Angrand and Mouthereau, 2021; Mouthereau et al., 2014; Muñoz, 1992; Teixell et al., 2018; Ford et al., 2022) and ~~. These deformations are~~is consistent with the exhumation ~~at ~85 Ma~~ of the Pelvoux crystalline basement to the northeast at ~85 Ma (Fig. 2; Boschetti et al., 2025a).

~~After~~ Following this tectonic change, marine incursions ~~only~~ were limited and localized ~~marine incursions occurred~~ from the Late Eocene to the Miocene (Fig. 2B). This period corresponds to the early Alpine collision, which affected the internal domains and the eastern parts of the External Crystalline Massifs (e. g. Ssimon-Labric et al., 2009; Boschetti et al., 2025c). Meanwhile, regional-scale extension developed in the European plate, driven by ~~due to the evolution of~~ the Western European Rift system and the opening of the Liguro–Provençal back-arc basin in southeastern France (Fig. 1) (Hippolyte et al., 1993; Séranne et al., 2021; Jolivet et al., 2021; Boschetti et al., 2023).

In the eastern ~~part of the~~ basin, the latest compressional phase is recorded by N–S to NW–SE-trending structures associated with the Digne thrust (Fig. 1-2) and final Alpine exhumation between ~12 and 6 Ma (Schwartz et al., 2017).

3. Sampling and methods

3.1 Sampling strategy

~~The s~~Sampling sites were carefully selected to characterize both the nature and ages of ~~the~~ brittle deformation ~~that~~ in ~~affecting~~ged the Jurassic and Cretaceous formations ~~within~~ of the Vocontian ~~basin~~ Basin (Fig. 2A). We first targeted sites where normal faults ~~The main structures~~ were described as syn-rift faults or veins formed shortly after deposition (~~were first identified based on the work of~~ Homberg et al.~~–~~, ~~(~~2013), and where we observed calcite mineralizations~~, who described syn-extensional features in the Vocontian Basin that were formed "shortly after" sediment deposition~~. The analysis of these specific sites was expanded to include other types of brittle structures, such as strike-slip and reverse faults, to document the polyphase deformation of the Vocontian Basin. ~~We~~ Our sampling targets were further guided using~~used~~ the 1:50.000 scale BRGM geological maps from Die to Sisteron ~~to select our sampling targets~~.

3.2 Tectonic and paleostress analysis

To reconstruct the tectonic evolution of brittle deformation in the Vocontian Basin, fault-slip data and other stress indicators, ~~like~~ including calcite veins, were measured in the field and collected for U-Pb dating. Local stress states were inferred by inverting fault-~~-~~slip data ~~using~~ following the methodology ~~outlined~~ of ~~by~~ Angelier (1990) using ~~, implemented in~~ the Win-Tensor software (Delvaux and Sperner, 2003). This analysis provided the orientation of the three principal stress axes (σ1, σ2, and σ3) and the shape of the stress ellipsoids defined by the ratio $\phi = \frac{\sigma 2-\sigma 3}{\sigma 1-\sigma 3}$, reflecting the relative magnitudes of the principal stresses. Relative chronology ~~between~~ of the reconstructed stress tensors was ~~achieved~~ determined ~~through~~ from cross-cutting relationships between successive generations of veins and faults (normal, reverse, or strike-slip faults). Chronology ~~with respect~~relative to folding was ~~further~~ refined by comparing the orientation of faults, veins, and/or associated stress states in their present-day ~~configuration~~ and ~~after~~ unfolded ~~unfolding~~configurations. This approach assumes that faults originally ~~were neo~~formed according to an Andersonian state of stress, with one principal stress axis ~~being~~ vertical.

3.3 Calcite U-Pb geochronology

Prior to U-Pb analyses, each polished thick section was petrographically characterized at IPRA (Institut Pluridisciplinaire de Recherche Appliquée) in Pau, France. This ~~characterization~~ involved ~~the use of an~~ optical microscopye coupled with cathodoluminescence (CL) imaging to identify multiple calcite generations (~~shown in~~ Supplementary~~.~~ Material~~.~~ Fig. S1). CL images were acquired using an OPEA Cathodyne system coupled with a Nikon BH2 microscope, operating at an acceleration voltage of 12.5 kV and an intensity of 300–500 mA. ~~The~~ U-Pb ~~absolute~~ dating of calcite was performed at IPREM laboratory (Institut des Sciences Analytiques et de Physico-Chimie pour l'Environnement et les Matériaux) ~~laboratory~~, following the ~~analytical approach described by~~protocol of Hoareau et al. (2021). This method employs isotopic mapping of U, Pb, and Th via a continuous ablation process, combined with a virtual spot method to construct Tera-Wasserburg (TW) plots (Hoareau et al., 2021, 2024). ~~A comprehensive~~ Detailed ~~description of the~~ analytical procedure and data processing is provided in the Supplementary Material 1 (Tabs.~~.~~ A1~~-, Tab.~~ A2). The ~~analytical~~ setup ~~included~~ used a 257 nm femtosecond laser ablation system (Lambda3, Nexeya, Bordeaux, France), operating at a frequency of 500 Hz with a spot size of 15 µm. Ablation was conducted in a controlled atmosphere composed of helium (600 mL/min) and nitrogen (10 mL/min), ~~which was subsequently~~ mixed with argon in the ICPMS. This system was coupled to an HR-ICPMS Element XR (ThermoFisher Scientific, Bremen, Germany) equipped with a jet interface (Donard et al., 2015).

3.4 Burial history

The subsidence history of the Vocontian Basin was reconstructed using stratigraphic sections, including thicknesses and lithologies, from the 1:50.000 scale geological maps of Die, Mens, Dieulefit, Luc-en-Diois, Gap, Nyons, Serres, Laragne-Montéglin, Vaison-la-Romaine, and Séderon, providing basin-wide coverage (Fig. 4). Standard backstripping techniques (Allen and Allen 2013) were applied ~~for this analysis~~. The sedimentary units were first decompacted using ~~a~~ coefficients ~~corresponding~~ appropriate to their dominant ~~main~~ lithology (limestone, marl or clay), ~~and~~ with stratigraphic ages inferred from the geological maps. To enable comparison between ~~the different sedimentary~~stratigraphic columns, the stratigraphic ~~columns~~ data were resampled ~~at regular temporal intervals, every~~at 1 Myr intervals, grouped into 5 Myr bins, ~~of 5 Myr~~ and ~~finally~~ interpolated using the 2D spline method.

3.5 RSCM thermometry approach

To determine the peak temperatures reached by sediments ~~and metasediments~~ in the Vocontian B~~b~~asin, ~~we conducted~~ RSCM analyses were conducted on an initial set of ~~rock samples collected from~~ Middle to Upper Jurassic and Lower Cretaceous carbonate samples collected~~s~~ ~~close~~ near ~~to~~ U-Pb dated calcites (Fig. 2A, 4). ~~For comparison, this set was complemented by~~ ~~a~~A second set of samples was ~~taken~~collected further east,~~wards~~ in~~,~~ or near,~~;~~ the Authon-Valavoire thrust nappe, a ~~(~~parautochtonous unit ~~below~~ at the front of the Digne nappe~~)~~, where ~~the~~ deeper Lower Jurassic strata of the Vocontian are exposed and diapirism has ~~been described~~occurred (e.g., Célini et al., 2024). The RSCM approach ~~is~~ constrains ~~used to understand~~ thermal processes ranging from advanced diagenesis to high-grade metamorphism, covering temperatures from 100 to 650°C (e.g., Ayoa et al., 2010; Koukestu et al., 2014; Schito et al., 2017). ~~Depending~~ Appropriate calibrations depend on the temperature range and ~~the~~ geological context~~, different calibrations are proposed~~. Here, ~~In this study,~~ we applied the calibration of Lahfid et al. (2010) ~~for~~ was applied for temperatures ~~ranging~~ between 200 and 340°C, and the qualitative approach ~~proposed~~ of ~~in~~ Saspiturry et al. (2020) for ~~lower~~ temperatures between 100 and 200°C. ~~The a~~Analyses were performed at the Bureau de Recherches Géologiques et Minières (BRGM; Orléans, France) using ~~. The Raman spectra were obtained with~~ a Horiba LABRAM HR instrument with a 514.5 nm solid-state laser source ~~for excitation~~. The laser ~~is~~ was focused ~~on the samples~~ with a BxFM microscope using a x100 objective with a numerical aperture of 0.90 and under 0.1 mW ~~on~~ at the sample surface.

4. Results

4.1 Microtectonics and paleostress reconstructions

Veins and striated planes associated with folds (Fig. 5A), reverse faults (Fig. 5B) and normal faults (Fig. 5C) were measured and sampled. Stereo~~dia~~grams of beddings, fault-slip data, veins and, when ~~necessary~~relevant, their associated back-tilting state of stress, are presented in Figure 6. When ~~the~~ sufficient ~~number of~~ fault-slip data ~~was sufficient~~were available for inversion (~~a~~ minimum of four ~~is required~~), the calculated stress axes ~~have been~~are reported (Fig. 6; Table 1). In this section, ~~we first present~~ data from samples VOC-23-09a to VOC-23-16d are presented ~~(~~in numerical order,~~)~~ followed by ~~and then introduces~~ samples BON-23-01 to ~~, 02, and~~ 03, ~~along with~~and GLAN-23-02, which~~.,~~ ~~which These samples~~ belong to a second, ~~and~~ separate field campaign. No measurements were conducted for samples VOC-23-01a and VOC-23-01b, as the sampling area ~~is~~ lies ~~located~~ within ~~a~~ the diapiric structure of the Dentelles de

Montmirail (Figs. 2A and, 6), whichpotentially could preventing a reliable interpretation of the paleostress tensorintroducinge local complexitiesy.

The sampling area of sample VOC-23-09b shows is a majoritydominated by of strike-slip faults, for whichwith paleostress inversion reveals indicating a strike-slip regime resolving under a NW-SE-directed compression (Fig. 6). At site of samplethe VOC-23-11a site, thewhere bedding is flat,. We resolve a strike-slip regime with pPpaleostress reconstructions also that indicatereveal a strike-slip regime, involving NE-SW compression and NW-SE extension (Figs. 5B, 6).

Samples VOC-23-12a and VOC-23-12b exhibit are suggestive ofrecord distinct deformation patterns. While sample VOC-23-12a corresponds comprises to calcite veins indicative of consistent with WNW-ESE extension, whereas sample VOC-23-12b exhibits similar calcite veins, together with as well as additional strike-slip deformation, consistent with as reported on the stereogram. This reflects WNW-ESE compression and NNE-SSW extension (Fig. 6). This stress orientation closely matches that of , which is not significantly different from our result in sample VOC-23-09a and b sites. The Considering theThe geometry of the stress axes, when considered alongside the dip and orientation ofrelative to the bedding dip and orientation suggests that this state of stress occurred afterpostdates folding.

Sample At the VOC-23-13 site, shows strike-slip faults that are consistentindicate a paleostress regime characterized by N-S-directed compression with anand E-W-directed extension and N-S-directed compression (Figs. 5C and ,6). Sample VOC-23-14a, represents is a calcite vein spatially that is associated with sample VOC-23-14b, occurs adjacent to ., which exhibits This vein is located alongside a strike-slip fault with with a sinistral component. Paleostress reconstruction indicates a WNW-ESE extension coupled withand NNE-SSW compression (Fig. 6).

Sample VOC-23-16d shows calcite veins affected by strike-slip deformation. In contrast, sample VOC-23-12b only shows only post-vein strike-slip deformation (post-vein) on the stereogram. Paleostress calculation analysis indicates an NW-SE-directed extension (Fig. 6). Samples BON-23-01a and BON-23-01b correspond consist ofto a striated calcite that has been affected by layer-parallel shortening (LPS), . This is interpreted as representing flexural slip during related to folding (Lacombe et al., 2021) (Figs. 5A, 6). Sample BON-23-01c, is a calcite vein that formed within the same fold, as the previous samples. It is interpreted to have formed during the fold growth of the fold. Paleostress analysis reconstruction of at the Bonneval outcrop indicates N20°E-directed compression associated with the formation of the N110°E-trending fold (Figs. 5A, 6). Finally, the GLAN-23-02 sample outcrop exhibits a normal fault coherent consistent with a NE-SW-oriented extension direction.

4.2 Petrography of calcite samples

In summarytotal, 15 samples were dated in this study: 6 veins (samples VOC-23-01a, 01b, 09b, 12a, 14b and BON-23-03) and 9 striated fault planes with striations (samples VOC-23-9a, 11a, 12b, 13, 14a, 16d, BON-23-01, 02 and GLAN-23-02). Most samples exhibit contain millimetric to centimetric blocky or to elongate-blocky calcite, in sizes ranging from millimetres to centimetres (Fig. 5;) (samples VOC-23-01, 9a, 12a, 22b, 13a, 14a, BON-23-01, 02, 03 and GLAN-23-02). They areThese calcites are characterized by homogeneous luminescence, indicating no evidence ofa single multi-phase calcite growth with no evidence of recrystallization (Figs. 7A, B; Supplementary. Material Fig. S1.). Two samples exhibit different distinct calcite morphologies. Sample VOC-23-11a contains a centimetric calcite showing with a transitional morphology between syntaxial and stretched crystalsing (Figs. 7C, D), . This suggestings the presence of crystals with variable growth planes orientations andwithin the fault plane, indicating potential multiple crack-seal events. Similarly, sample VOC-23-16d displays millimetric to centimetric blocky calcite. This is, predominantly composed of blocky calcite, which and appears to be crosscut by a secondyounger generation of more elongated and stretched second calcite generation (Fig. 7C, D).

4.3 Calcite U-Pb geochronology

This study presents 16 new calcite U-Pb ages obtained from eight types of brittle structures (Table 1; Figs. 8, 9, 10). The Tera-Wasserburg diagrams show data well spread along the discordia line, with . The Mean Squared Weighted Deviation (MSWD) ranginges from 1.1 to 1.9, which indicating robust is consistent withand well-resolved age estimates. Three distinct age groups can be identified from within this the dataset.

The first age group corresponds to the Late Cretaceous to Early Eocene periods interval, based on from veins collected in late Jurassic-Early Cretaceous strata in the Westwestern part of the basin. Ages obtained inIn the “Dentelles de Montmirail” area, ages are of 82.9 ± 3.8 Ma (sample VOC-23-01b) and 76.5 ± 3.4 Ma (sample VOC-23-01a) were obtained. Further north, Inin the Die region, tTo the North north of the study area, in the Die region, corresponding fold-related structures associated with N20°E shortening are have been datedyielded ages to of 72.0 ± 3.7 Ma (sample BON-23-01a), 71.2 ± 8.1 Ma (sample BON-23-01b), and 50.0 ± 4.3 Ma (sample BON-23-01c) (Fig. 8).

The second age group corresponds to veins and faults ~~dated~~ formed during ~~back to~~ the Oligocene. The o~~O~~btained ages range from 34.3 ± 1.5 Ma (vein: VOC.23.14a), 30.3 ± 1.5 Ma (fault: VOC.23.14b2), 30.0 ± 2.8 Ma (fault: VOC.23.13b), 28.1 ± 1.2 Ma (fault: VOC.23.14b1), 25.6 ± 1.3 Ma (vein: VOC.23.12a), 23.2 ± 1.3 Ma (deformed vein: VOC.23.12a and b) and 27.6 ± 5.4 Ma (fault: GLAN.23.02) (Fig. 9). Most of these fractures correspond to ~~an~~ NW-SE to NE-SW extension (Fig. 6). However, o~~One of them~~ ~~,~~ sample VOC.23.12b indicates ~~, which is the same kind of veins as VOC.23.12a, is consistent with~~ a strike-slip stress regime with NNE-SSW extension and WNW-ESE compression, similar to that inferred from ~~sample~~ VOC.23.09 (Fig. 6). Calcite veins in VOC.23.12b ~~is~~are of the same ~~kind~~type ~~of veins~~ as those in VOC.23.12a. ~~,~~

The third age group corresponds to Miocene veins and strike-slip faults ~~collected~~ hosted in Upper Jurassic-lower Cretaceous carbonates. Two subgroups can be distinguished. The first subgroup, ~~characterized by ages of~~dated to 12.2 ± 3.2 Ma and 12.5 ± 5.2 Ma (fault: VOC.23.11a and fault: VOC.23.16d), ~~is~~ records a ~~associated with a~~ strike-slip regime ~~consistent~~ defined ~~with~~ by NE-SW compression and NW-SE extension (Figs. 10, 6). The second subgroup, ~~defined~~ with ~~by~~ ages of 7.8 ± 0.6 Ma and 7.0 ± 2.2 Ma (fault: VOC.23.09a and vein: VOC.23.09b), also ~~corresponds~~ reflects ~~to~~ a strike-slip regime but ~~corresponds~~ with ~~to~~ stress orientations indicating NW-SE compression and NE-SW extension (Figs. 10, 6).

4.5 RSCM thermometry

RSCM data from the first set of Upper Jurassic and Lower Cretaceous carbonates in the central and southern parts of the ~~studied~~ study area indicate ~~that~~ maximum temperatures ~~did not exceed~~below 100°C (~~samples~~ VOC-23-01 and VOC-23-16; Table 2). For the second set~~ of samples~~, reliable temperatures ~~were~~ estimates ~~successfully determined~~were obtained for 12 samples using an appropriate calibration (Table 2, Fig. 6), which can be divided in two ~~sub~~groups. Temperatures measured in Lower to Upper Jurassic strata ~~sampled~~ near Saint Roman and Montmaure, in the Die area, ~~display the lowest temperatures~~ range~~ing~~ between 100 and 180°C (~~samples~~ VOC-~~18~~23-~~17~~18, VOC-~~18~~23-17~~8~~).~~,~~ The lowest temperatures are found near Veynes and close to the Devoluy massif (sample VOC-~~18~~24-20), in Sigoyer village (samples VOC-~~18~~23-02~~21~~, VOC-~~18~~23-~~22~~03), and in the upper stratigraphic unit of the Authon-Valavoire nappe (~~sample~~ VOC-~~18~~24-28), and in the eastern part of the basin, below ~~this~~ the Digne nappe (sample VOC-~~18~~24-29). The higher bound of RSCM temperatures, reaching up to ~~a~~t 170°C, is measured ~~for~~ in samples VOC-~~18~~24-24a and 33, both located near diapiric structures~~:~~ ~~(~~“Rocher de Hongrie”~~;~~ (~~(~~Célini et al., 2024). These ~~latter~~ values align ~~are consistent~~

with previously reported temperatures ~~between~~ of 140- ~~and~~ 200°C ~~recently published~~ in the vicinity of ~~this~~ the same diapir (Célini et al., 2024). The second ~~sub~~group ~~defined~~ characterized by higher temperatures between 215 and 275°C, includes ~~are~~ samples located ~~found~~ 1 km to the south of Sigoyer (~~sample~~ VOC-~~18~~24-23), within the middle Jurassic ~~layers~~ strata in the hangingwall of the Authon-Valavoire nappe (~~sample~~ VOC-~~18~~24-25), and in the Lias strata sequence near the Astoin diapir (~~sample~~ VOC-~~18~~23-31). Temperatures of this second ~~sub~~group fall within the temperature range recorded in the Authon-Valavoire nappe, particularly near Astoin, closer to the Digne nappe~~,~~ ~~near Astoin~~ (Célini et al., 2024). To summarize, our data reveal a thermal contrast between the western and eastern domains of the Vocontian B~~b~~asin. While the organic matter of upper Jurassic-lower Cretaceous formations ~~is~~ remaines thermally immature, deeper Early-Middle-Late Jurassic formations exposed in the eastern part of the Vocontian basin, close to the Authon-Vallavoire and Digne nappes ~~show~~ exhibit significantly higher thermal maturity, with RSCM temperatures exceeding 180°C and reaching up to 275°C. ~~The shift towards higher~~A similar increase in RSCM temperatures between the Upper Jurassic-Early Cretaceous and deeper stratigraphic units of the Early-Middle Jurassic has also been ~~observed~~ documented in stratigraphic ~~columns~~ sections ~~analysed from~~of the Digne Nappe (Célini et al., 2022; Balansa et al., 2023).

4.4 Burial histories and temperatures reached in the basin

Burial histories for the Vocontian Basin are presented in Figure 11. Each curve represents the burial evolution within the basin, ~~calculated~~ reconstructed from ~~from a synthesis of~~ stratigraphic thicknesses indicated in explanatory notes of ~~inferred from~~ the BRGM 1/50.000 geological maps covering the basin. The data indicate ~~A first observation is~~ that ~~the~~ total sediment accumulation ~~in the Vocontian basin appears to have~~ reached a maximum of 6-7 km since the Early Jurassic. This is shown by the ~~estimated~~ decompacted thicknesses estimated ~~of~~ at 6800 m in the Die region and ~~, or~~ 5900 m ~~in~~ near Nyons, in the northern and western ~~parts~~ sectors of the basin, respectively. In contrast, areas lacking exposures of ~~In regions of the basin where the~~ L~~l~~ower Jurassic series such as Vaison-la-Romaine, show ~~are not exposed the total~~reduced total subsidence ~~is obviously lower; it is~~of ~~only~~ around 2500 m ~~in the region of Vaison-la-Romaine~~. Despite these differences, most ~~regions~~ parts of the basin recorded a main phase of burial during the Middle Jurassic~~, in the~~ (Callovian, ~~~about~~ 160 Ma ~~(Fig. 11~~), associated with the widespread~~.~~ ~~This phase affected the entire Vocontian Basin. It is shown by the~~ deposition of marls ~~to~~ and shales ~~deposits~~ of the “Terres Noires”, ~~facies characteristic~~typical of the External Alps. During this period, about 2 km of “Terres Noires” ~~were deposited (accumulation~~accumulated with rates of 200-400 m/Myr). After Following the Middle Jurassic, the burial slowed rates decreased down but continued throughout the Late Jurassic and Early Cretaceous. A second phase of accelerated subsidence took place during the Early Cretaceous, around 130 Ma (, in the Hauterivian), documented . It is documented in the Mens section by the deposition of about 700 m of marls and limestones (Fig. 4). A third main major burial phase, of burial is recorded arounddated to 100-90 Ma (Fig. 11), is recorded in the 6 out of the 10 stratigraphic sections (Fig. 11). It isThis phase is characterized by increasing siliciclastic influx, revealed by the deposition of 700-800 m sandstones alternating sandstones, with marls and limestones with a thickness of about 700-800 m (e.g., Nyons, Sédéron, Vaison-la-Romaine) (Fig. 10). In contrast, The the Gap, Laragne-Montéglin, and Mens sections, however, record show evidence of erosion rather than sedimentation at this time. These contrasting depositional patterns reveal concurrent both uplift in the source regions and structural compartmentalization in the Vocontian basin Basin (Fig. 11). A last episode of subsidence, reaching of maximum 350-500 m (e.g., Die, Laragne) is documented during the Eocene-Oligocene (Fig. 11).

5. Discussion

The results from this study are put into perspective of the evolution of the Vocontian Basin of south-east France through time. For this, we merge results from structural analysis with corresponding U-Pb calcite ages, and discuss the evolution of the related burial history estimated from the lithological logs, which have been used to infer paleo-thermal gradients. Four main evolutionary stages can be proposed based on these data, which are discussed below.

5.

5.1 The Vocontian basin at the time of Mesozoic rifting: E-W trend in thermal gradients and low Ca-rich fluid circulation (170-90 Ma)

The Vocontian basin recorded a prolonged phase of subsidence during throughout the Jurassic and Cretaceous (Fig. 11), which is was however not associated with a distinct fluid event. This period coincides with the rifting of the European paleomargin as inferred by the thermal evolution of the Pelvoux Variscan crystalline basement to the north of the Pelvoux massif (Boschetti et al., 2025a,c) to the North, and from the burial history below the Digne Nappe to the east (Célini et al., 2023), which bounds the Vocontian to the east. This latter eEastern rim margin of the basin was likely inverted during the late stages of the Alpine collision between 12 and 6 Ma (Schwartz et al., 2017). We distinguish a first major phase of sedimentary burial that occurred during the Callovian-Oxfordian (, between 170- and 160 Ma), which postdates. It This burial postdates the necking of the European paleomargin, which occurred during rifting,

~~as~~ identified in the External Crystalline Massifs (Mohn et al., 2014; Ribes et al., 2020; Dall'Asta et al., 2022) and is ~~is~~ synchronous with the opening of the Alpine Tethys (Lemoine et al., 1986~~7~~; Manatschal and Müntener, 2009). ~~It~~ This rifting is recognized in the Vocontian ~~basin~~Basin, where it is expressed by WNW–ESE extension ~~across the entire basin~~ (Dardeau et al., 1988; Homberg et al., 2013), but it is not ~~recorded~~ captured in our calcite U-Pb ages. Similar observations can be made for the subsequent extensional Cretaceous ~~event at around~~(~ ~~–~~135 Ma), for which no faults of that age ~~is~~ are reported. The high temperatures measured ~~in the Vocontian basin of~~in the Digne Nappe at this time are interpreted ~~to~~ as reflecting renewed extension associated with the opening ~~in the basin as~~of the Valaisan domain ~~opened~~ along the European margin (Célini et al., 2023), consistent with ~~continuous~~ ongoing burial heating recorded in the Pelvoux massif (Boschetti et al, 2025a,c). This thermal ~~new~~ peak ~~in sedimentation is consistent~~coincides with a shift from the Middle Jurassic WNW–ESE extension to NNE–SSW extension ~~al regime~~ during the Barremian– ~~-to~~ Aptian ~~interval~~ (Dardeau, 1988; de Graciansky and Lemoine, 1988; Homberg et al., 2010). This later extensional ~~event~~ phase is recorded not only throughout the Vocontian Basin (Homberg et al., 2013), but also along its margins. Evidence for this later extensional event includes deformation along the Ventoux–Lure fault zone (Beaudoin et al., 1986; Huang et al., 1988), the ~~development~~ formation of large-scale sliding domains on the Vercors platform (Bièvre and Quesne, 2004), and subsidence in ~~E~~east–~~W~~west-oriented domains along the Ardèche margin during the same period (Cotillon et al., 1979). Our RSCM analyses ~~show~~ indicate an increase ~~of~~ in peak temperatures ~~towards~~ toward the ~~East~~ east of the Vocontian Basin, where ~~the~~ deeper Lower Jurassic stratigraphic ~~series~~ strata ~~are~~ ~~is~~are exposed (Fig. 6; Table 2). ~~When we compared~~ Comparing ~~to corresponding burial~~these temperatures with temperature inferred from burial ~~estimates~~ depths~~ranging~~ ~~from~~ using normal (30°C/km) to high (60°C/km) geothermal gradients suggests ~~, we infer~~ that ~~our~~ the eastern sector ~~RSCM data reveal~~experienced unusually high to extreme gradients ~~in the East~~east, ~~that is,i.e. in the~~consistent with ~~direction of~~ increasing crustal thinning in the Vocontian-Valaisan rift segment this direction (Fig. 6; Table 2). It should be n~~N~~oted that the sharp increase in the geothermal gradients is not ~~necessarily entire~~solely ~~related~~ due to crustal thinning, but is also largely a ~~response~~ result of mantle thinning and asthenosphere ~~uprising~~uplift. The ~~lack~~ absence of calcite mineralisation in brittle tectonic features at this ~~age~~ time, despite specifically targeting potentially related veins, ~~in brittle tectonic features~~ is intriguing. Indeed, evidence of ~~mineralization of~~ barite, authigenic quartz and pyrite mineralization in the Callovian-Oxfordian shales in the deeper part of the basin is interpreted as reflecting basal fluid flow during syn-rift peak burial in the Middle Cretaceous, as well as brines related to salt diapirs (Guilhaumou et al., 1996). We suggest that the absence of Middle Cretaceous calcites can reflectscan be explained either the fact thateitherby 1) that faulting occurringed at a depth too shallow for calcite precipitation, and/or 2) that subsequent burial to a depth of 2-3 km, in the East,eastern basin leadingd to the dissolution of previous Middle Cretaceous calcites in responsedue to changing physical conditions (e.g., pH and, temperature). . In addition, mechanical decoupling in the Triassic salt layer during extension may have resulted in the localizationfocused of fluid flow, so that mineralized fluids of this age are detectable only locally, near the emergence of salt diapirs. and deformation at the base of the basin.

A third depositional phase occurred around 100-90 Ma, in agreement with syn-faulting deposits along the Clausis and Glandage fault systems in the Vocontian/Dévoluy basin (Fig. 11, 3) (Gidon et al., 1970; Arnaud et al., 1974) and with strike-slip motions activity along the Toulourenc faults in the Ventoux-Lure massif (Montenat et al., 2004). Regionally, On a broader scale, this tectonic phase coincides with strike-slip movements along the Cevennes, Nîmes and Durance faults (Montenat et al., 2004; Parizot et al., 2022), possibly potentially associated with local compression related to diapiric movement at 95-90 Ma (Bilau et al., 2023b) and normal faulting reported in Provence (Zeboudj et al., 2025). This episode is a response of the continental rifting between Iberia-Ebro and European plates, and the formation of the Pyrenean rift system (Angrand and Mouthereau, 2021) -(Fig. 12A). . It should be reminded that tThe locally complex tectonic evolution of SE France during the Middle-Late Cretaceous is a response to large-scale differential movements between Iberia-Ebro and Adria that accommodated both extension in the Pyrenees-Provence rift and contraction in the Alps (e.g., Le Breton et al., 2021; Angrand and Mouthereau, 2021; Boschetti et al., 2025b, In Press). Strike-slip movements along inherited faults (Cevennes, Nîmes, Durance faults) were associated with oblique extension accommodated by overlapping rift segments in the Pyrenean and Vocontian basins (Fig. 12). This complex tectonic setting likely triggered the emergence of continental blocks that can explain the abundance of sandstone deposits during this period in the Vocontian basin (Fig. 4, 11). This interpretation aligns with the documented formation of an uplifted structure in Provence during the Albian-Cenomanian, known as the Durancian Isthmus (Combes, 1990; Guyonnet-Benaize et al., 2010; Chanvry et al., 2020, Marchand et al., 2021). Cooling and exhumation in the French Massif Central to the west are also documented from 120-90 Ma (Olivetti et al., 2016), which may have contributed to feeding of the Vocontian basin during this period (Fig. 12A). Although this period is synchronous with the onset of Adria/Europe convergence (e.g., Le Breton et al., 2021; Angrand and Mouthereau, 2021;

Boschetti et al., 2025a,b,c), the impact of contraction in the Alps on the evolution Vocontian Basin remains to be assessed. It should be reminded that the locally complex tectonic evolution of SE France during the Middle-Late Cretaceous is a response to large-scale differential movements between Iberia-Ebro and Adria that accommodated both extension in the Pyrenees-Provence rift and contraction in the Alps (e.g., Le Breton et al., 2021; Angrand and Mouthereau, 2021; Boschetti et al., 2025, In Press).

5.2 Post-Mid Cretaceous evolution of the Vocontian basinBasin: U-Pb/calcite dating record of multiple Pyrenean-Provençal collision events (90-34 Ma)collision and rifting events in the basins of south-east SE Francebasins of France

The oldest calcite U-Pb ages of 84.6 ± 2.4 Ma and 77.7 ± 2.9 Ma, reported in the Jurassic strata forming the wall of the Suzette diapir in the(“Dentelles de Montmirail”)structure are close to previously obtained ages of 90.6 ± 2.4 Ma of Bilau et al. (2023b), and are consistentalign with the age of the onset of the Pyreneanes-Provençalce collision dated around 84 Ma (Angrand and Mouthereau, 2021; Mouthereau et al., 2014; Muñoz, 1992; Teixell et al., 2018; Ford et al., 2022). Those These old calcite ages are likelymay reflect to be realed to the combined halokinetic movement of the Suzette diapir in response to far-field stresses that triggered tectonic inversion and exhumation all over Europe (Mouthereau et al., 2021). These ages can also be related to a deformation event folding along E-W trending folds in the Dévoluy massif , affecting the Early Cretaceous units, and linked to associated to E-W-directed folding and erosional surface dated to Coniacian-Santonian (Fig. 3B) (ca. 85 Ma) (Flandrin, 1966; Lemoine, 1972; Gidon et al., 1970; Arnaud et al., 1974), or the end of diapiric movement during extension in southern Provence (Wicker and Ford, 2021). Younger U/Pb ages of 72.0 ± 3.7 Ma and 71.2 ± 8.1 Ma associated with N20°E shortening coincides with the intensification of the In the Pyrenees exhumation seems to increase fromat 75-70 Ma (Mouthereau et al., 2014), a phase that and this is recorded regionally recorded across southeastern in SE of France by the a cooling event documented from of the Pelvoux to the Maures-Tanneron massifs (Fig. 12A) (Boschetti et al., 2025a,b In Press). It is also recognized in the region associated with the sinistral reactivation of the Cevennes fault around 76 Ma (Parizot et al., 2021). The Pyrenean-Provençal collision is therefore well represented in the Vocontian Basin. This timing is further in line with the earliest surface sediment cover deformation, which is recorded around 75 Ma (Parizot et al., 2021). U/Pb ages of 72.0 ± 3.7 Ma and 71.2 ± 8.1 Ma associated with folding during N20°E compression are consistent with the latest sinistral reactivation of the Cevennes

~~fault from since 76 Ma (Parizot et al., 2021). These ages can may also be related to folding along an Eeast-Wwest axis in the Dévoluy massif, affecting the Early Lower Cretaceous units. and This folding is associated to an erosional surface estimated, which formed to occur during the Turonian-Coniacian-Santonian period (ca. 85 Ma) (Fig. 3) (ca. 85 Ma) (Flandrin, 1966; Lemoine, 1972; Gidon et al., 1970; Arnaud et al., 1974).~~

Our data also resolve ~~another~~ a ~~later~~ younger N20°E-directed contractional stage dated at 50.0 ± 4.3 Ma (Fig. 6) that we link to the main Pyrenan-Provençal collision phase.~~.~~ ~~It~~ It is ~~well~~ recognized ~~identified also~~ in other ~~the~~ U/Pb age dataset ~~in~~ from Provence ~~in the U/Pb age dataset~~ (Zeboudj et al., 2025), and corresponds to a ~~N~~north-~~S~~ south compression ~~ive phase~~ spanning from 59 to 34 Ma~~. This stage is~~ regarded as the culmination of the Pyrenean-Provençal collision caused by plate-scale dynamic changes (Bestani et al., 2016; Balansa et al., 2022; Vacherat et al., 2016; Mouthereau et al., 2014; 2021) (Fig. 12B).~~. This episode is related to the acceleration of the collision process at around ca. 50 Ma, which was caused by dynamic changes in the motion of Africa motion, and the opening of the North Altantic ocean opening (e.g. Mouthereau et al., 2021).~~ In northwestern Europe, the Eocene also ~~also~~ heralds ~~announces~~ the onset ~~of opening of the aborted rift system~~ of the West European Rift (WER), which was active until the Oligocene and just precedes the opening of the Gulf of Lion (e.g. Séranne et al., 1999; Dèzes et al., 2004; Mouthereau et al., 2021).

5.3 Oligocene rifting related to the West European Rift development (35-23 Ma)

The WER stage is ~~well~~ represented in ~~the Vocontian basin~~our dataset ~~as indicated~~ by eight U/Pb dates ranging from 30.4 ± 2.7 to 24.3 ± 1.3 Ma associated with NW-SE to NE-SW extension (Fig. 12C). They ~~, which~~ coincide~~s~~ with ~~an~~ the extensional phase (35–23 Ma) ~~also~~ documented in Provence, W~~w~~estern Alps, E~~e~~astern Pyrenees, and Valencia Trough ~~, coeval with the late activities of the West European Rift~~ (Merle and Michon, 2001; Ziegler and Dèzes, 2006). ~~In our study region, the shallow depth of iso-velocity contour Vs=4.2 km.s^{-1}, considered to be a proxy for the Moho (Schwartz et al., 2024), confirms a significant crustal thinning in the Valence-Rhone depression (Fig. S21, Supplementary Material 1). It should also be noted that the~~The Late Eocene-Early Oligocene period also coincide~~s~~d with the onset ~~of deposition in the~~of the ~~flexural basin of the~~ Alpine foreland (Ford et al., 1999).~~.~~ The flexural bending ~~deflection~~ of the European margin caused by Alpine loading ~~is~~ likely ~~increasing~~ increased ~~the~~ extensional stresses in the foreland, ~~associated~~ where ~~with~~ the WER formed, however the available data are insufficient to draw defitinive conclusions. From Chattian-Aquitanian times, at ca. 23 Ma, the opening of the Gulf of Lion~~s~~ and of the Ligurian basin (e.g., Séranne et al., 1999; Jolivet et al., 1999, 2020) ~~commenced~~ initiated following the demise of the WER suggesting a tectonic relationship between these two rifting events (Mouthereau et al., 2021) (Fig. 12C). In our study area, the shallow depth of the iso-velocity contour Vs=4.2 $km.s^{-1}$, considered to be a proxy for the Moho (Schwartz et al., 2024), and the 3D geological modelling (Bienveignant et al., 2024), confirms a significant crustal thinning in the Valence-Rhône depression, where structures related to the WER are preserved (Fig. S2, Supplementary Material 1). The excellent preservation of the Oligocene-Miocene extensional phase in our dataset suggests a positive feedback~~s~~ between crustal thinning (Fig. S2~~1~~, Supplementary Material 1) and physical conditions that bec~~o~~ame favourable ~~to~~ for calcite precipitation ~~closer~~ at shallower depths~~to the surface~~, as the basin was progressively exhumed ~~during~~ following ~~the former~~ Late Cretaceous shortening.

5.4 Alpine collision and fold and thrust belt propagation (<16 Ma)

The youngest calcite U/Pb ages of 12.2 ± 3.2 Ma, 12.5 ± 5.2 Ma, 7.8 ± 0.6 Ma and 7.0 ± 2.2 Ma are associated with NE-SW compression. This result agrees with the westward propagation of the Alpine deformation front, which migrated forelandward from 16~~5~~ to 7 Ma in the Vercors massif (Bilau et al., 2023a; Mai Yung Sen et al., 2025) to the north of the Vocontian Basin (Fig. 12D). This timing also coincides with the exhumation of Alpine ~~external crystalline massifs~~basement, such as the Belledonne and Pelvoux massifs~~-~~, which accelerated at ca. 12 Ma (e.g. Beucher et al., 2012; Girault et al., 2022; Boschetti et al., 2025a). This age range is also is agreement with the Digne Nappe emplacement at 13-9 Ma (Schwartz et al., 2017) and fold and thrust development in the frontal southern Alps between 18.2 ± 1.1 Ma and 3.16 ± 0.47 Ma obtained (Bauer et al., 2025 ; Tigroudja et al., 2025).

CONCLUSION

The goal of this study was to provide a refined chronology of deformation in the Vocontian Basin using an integrated approach combining U-Pb calcite geochronology, RSCM thermometry, and subsidence analysis. First, this study highlights the absence of mid-Cretaceous syn-rift calcites associated with the opening of the Vocontian Basin. This is possibly related to dissolution during subsequent burial, or reflect the localization of fluid flow and strain in the basal Triassic salt layer during the mid-Cretaceous extension. The temporal distribution of dated brittle structures reveals three main deformation episodes: (1) Late Cretaceous to Paleocene calcite precipitation associated with Pyrenean-Provençal convergence and diapirism; (2) Oligocene extensional phases tied to the West European Rift opening; and (3) Miocene strike-slip reactivation and contraction linked to the Alpine orogeny. These events are superimposed onto a long-term subsidence history that records major burial phases during the Jurassic and Cretaceous. Thermal data from RSCM analyses delineate a sharp eastward increase in geothermal gradients, suggesting enhanced crustal thinning and/or diapiric activity in the eastern part of the basin. This work highlights the possible mismatcha good coherence between of the local deformation the tectonic evolution of a region and the tectonic history inferred inferred from calcite U–Pb dating and -and paleostress analysis, andand of the regional tectonic evolution. The calcite U– Pb ages, which is are sensibtivle to the brittle behaviour of the sedimentary cover and to combined fluid circulation during burial, history andas well as to the specific physical conditions required to for the precipitation ofe syn-deformation calcite. This makes it impossible to document the fluid-free brittle history.

Declaration of Competing Interest

The authors declare that they have no known competing financial interests or personal relationships that could have appeared to influence the work reported in this paper.

Availability of data material

The dataset(s) supporting the conclusions of this article is(are) available in Supplementary Material 1.

Acknowledgments

Authors would like to thank BRGM and the RGF program which allows the founding this project.

Author’s contribution

LB is the corresponding author who carried out the field investigation, analysis, interpretation and drafting of the manuscript. MP carried out the field investigations, analysis and review of the manuscript. FM carried out the filed investigation, interpretation, drafting a review of the manuscript. GH carried out the U-Pb analysis and review of the Manuscript. SS and YR carried out the field investigation and review of the manuscript. DB carried out interpretation and discussion and AL carried out analysis of Raman data.

Funding

This study was made possible thanks to ministerial funding from the SDU2E doctoral school at Toulouse University and by additional the funding by the RFG-Alps programme, coordinated by the BRGM.

References

Allen, P. A., & Allen, J. R.: Basin analysis: Principles and application to petroleum play assessment. John Wiley & Sons, 2013.

Angelier, J.: Inversion of field data in fault tectonics to obtain the regional stress—III. A new rapid direct inversion method by analytical means. Geophysical Journal International, 103(2), 363-376.https://doi.org/10.1111/j.1365-246X.1990.tb01777.x, 1990.

Angrand, P., & Mouthereau, F.: Evolution of the Alpine orogenic belts in the Western Mediterranean region as resolved by the kinematics of the Europe-Africa diffuse plate boundary. BSGF-Earth Sciences Bulletin, 192(1), 42. https://doi.org/10.1051/bsgf/2021031, 2021.

Arnaud H., Charollais J., Delamette M. & Portault B. : Crétacé supérieur. Chaînes subalpines. In: S. Debrand-Passard et al., Eds, Syn thèse géo lo gique du Sud-Est de la France. – Mém.BRGM, 125, 355-359, 1984.

Balansa, J., Espurt, N., Hippolyte, J. C., Philip, J., & Caritg, S.: Structural evolution of the superimposed Provençal and Subalpine fold-thrust belts (SE France). Earth-Science Reviews, 227, 103972. https://doi.org/10.1016/j.earscirev.2022.103972, 2022.

Balansa, J., Lahfid, A., Espurt, N., Hippolyte, J. C., Henry, P., Caritg, S., & Fasentieux, B.: Unraveling the eroded units of mountain belts using RSCM thermometry and cross-section balancing: example of the southwestern French Alps. International Journal of Earth Sciences, 112(2), 443-458. https://doi.org/10.1007/s00531-022-02257-3, 2023.

Bauer, R., Corsini, M., Matonti, C., Bosch, D., Bruguier, O., & Issautier, B.: The role of Cretaceous tectonics in the present-day architecture of the Nice arc (Western Subalpine foreland, France). Journal of Structural Geology, 105538, 2025.

Bestani, L., Espurt, N., Lamarche, J., Bellier, O., & Hollender, F.: Reconstruction of the Provence Chain evolution, southeastern France. Tectonics, 35(6), 1506-1525-https://doi.org/10.1002/2016TC004115, 2016.

Beaudoin, B., Friès, G., Joseph, P., Bouchet, R., & Cabrol, C. : Tectonique synsédimentaire crétacée à l'ouest de la Durance (S.-E. France). Comptes rendus de l'Académie des sciences. Série 2, Mécanique, Physique, Chimie, Sciences de l'univers, Sciences de la Terre, 303(8), 713-718, 1986.

Beucher, R., van der Beek, P., Braun, J., & Batt, G. E.: Exhumation and relief development in the Pelvoux and Dora-Maira massifs (Western Alps) assessed by spectral analysis and inversion of thermochronological age transects. Journal of Geophysical Research: Earth Surface, 117(F3). https://doi.org/10.1029/2011JF002240, 2012.

Bièvre, G., & Quesne, D.:Synsedimentary collapse on a carbonate platform margin µ (lower Barremian, southern Vercors, SE France). Geodiversitas, 26(2), 169-184, 2004.

Bienveignant, D., Nouibat, A., Sue, C., Rolland, Y., Schwartz, S., Bernet, M., Dumont, T., Nomade, J., Caritg, S., & Walpersdorf, A.: Shaping the crustal structure of the SW-Alpine Foreland : Insight from 3D modeling. Tectonophysics, 889, 230471. https://doi.org/10.1016/j.tecto.2024.230471, 2024.

Bilau, A., Bienveignant, D., Rolland, Y., Schwartz, S., Godeau, N., Guihou, A., et al.: The Tertiary structuration of the Western Subalpine foreland deciphered by calcite-filled faults and veins. Earth Science Reviews, 236, 104270, 2023a.

~~Bilau, A., Bienveignant, D., Rolland, Y., Schwartz, S., Godeau, N., Guihou, A., ... & Dumont, T. (2023a). The Tertiary structuration of the Western Subalpine foreland deciphered by calcite-filled faults and veins. *Earth Science Reviews*, *236*, 104270.~~

Bilau, A., Rolland, Y., Dumont, T., Schwartz, S., Godeau, N., Guihou, A., & Deschamps, P., 2023b. Early onset of Pyrenean collision (97–90 Ma) evidenced by U–Pb dating on calcite (Provence, SE France). Terra Nova, 35(5), 413-423. https://doi.org/10.1111/ter.12665, 2004

Boschetti, L., Schwartz, S., Rolland, Y., Dumont, T., and Nouibat, A.: A new tomographic-petrological model for the Ligurian-Provence back-arc basin (North-Western Mediterranean Sea), Tectonophysics, 230111, https://doi.org/10.1016/j.tecto.2023.230111, 2023.~~Boschetti, L., Schwartz, S., Rolland, Y., Dumont, T., & Nouibat, A. (2023). A new tomographic-petrological model for the Ligurian-Provence back-arc basin (North-Western Mediterranean Sea). *Tectonophysics*, *868*, 230111.~~

Boschetti, L., Mouthereau, F., Schwartz, S., Rolland, Y., Bernet, M., Balvay, M., ... & Lahfid, A.: Thermochronology of the western Alps (Pelvoux massif) reveals the longterm multiphase tectonic history of the European paleomargin. Tectonics, 44(2), e2024TC008498. https://doi.org/10.1029/2024TC008498, 2025a.

Boschetti, L., Rolland, Y., Mouthereau, F., Schwartz, S., Milesi, G., Munch, P., Bernet, M., Balvay, M., Thiéblemont, D., Bonno, M., Martin, C., and Monié, P.: Thermochronology of the Maures-Tanneron crystalline basement: insights for SW Europe Triassic to Miocene tectonic history, Swiss J. Geosci., 118, 14, https://doi.org/10.1186/s00015-025-00485-8, 2025b.~~Boschetti, L., Rolland, Y., Mouthereau, F., Schwartz, S., Milesi, G., Munch, P., Bernet, M., Balvay, M., Thiéblemont, D., Bonno, M., Martin, C. Monié, P.: Thermochronology of the Maures-Tanneron crystalline basement: Insights for SW Europe Triassic to Miocene tectonic history. Swiss Journal of Geoscience. https://doi.org/10.1186/s00015-025-00485-8, In Press~~

Boschetti, L., Boullerne, C., Rolland, Y., Schwartz, S., Milesi, G., Bienveignant, D., et al. Shear zone memory revealed by in-situ Rb-Sr and 40Ar/39Ar dating of Pyrenean and Alpine tectonic phases in the external Alps. *Lithos*, 108168, 2025c.

Célini, N. : Le rôle des évaporites dans l'évolution tectonique du front alpin: le cas de la nappe de Digne (Doctoral dissertation, Université de Pau et des Pays de l'Adour), 2020.

Célini, N., Mouthereau, F., Lahfid, A., Gout, C., and Callot, J.-P.: Rift thermal inheritance in the SW Alps (France): insights from RSCM thermometry and 1D thermal numerical modelling, Solid Earth, 14, 1–16, https://doi.org/10.5194/se-14-1-2023, 2023.~~Célini, N., Mouthereau, F., Lahfid, A., Gout, C., & Callot, J. P. (2023). Rift thermal inheritance in the SW Alps (France): insights from RSCM thermometry and 1D thermal numerical modelling. *Solid earth*, *14*(1), 1-16.Célini, N., Pichat, A., Mouthereau, F., Ringenbach, J. C., & Callot, J. P.: Along-strike~~

~~variations of structural style in the external Western Alps (France): Review, insights from analogue models and the role of salt. Journal of Structural Geology, 105048. https://doi.org/10.1016/j.jsg.2023.105048, 2023.~~

Célini, N., Pichat, A., Mouthereau, F., Ringenbach, J. C., & Callot, J. P.: Along-strike variations of structural style in the external Western Alps (France): Review, insights from analogue models and the role of salt. Journal of Structural Geology, 179, 105048. https://doi.org/10.1016/j.jsg.2023.105048, 2024.

Chanvry, E., Marchand, E., Lopez, M., Séranne, M., Le Saout, G., & Vinches, M. :

Tectonic and climate control on allochthonous bauxite deposition. Example from the mid-Cretaceous Villeveyrac basin, southern France. Sedimentary Geology, 407, 105727. https://doi.org/10.1016/j.sedgeo.2020.105727, 2020.

Combes, P. J. : Typologie, cadre géodynamique et genèse des bauxites françaises. Geodinamica Acta, 4(2), 91-109. https://doi.org/10.1080/09853111.1990.11105202, 1990.

Cotillon, P., Ferry, S., Busnardo, R., Lafarge, D., & Renaud, B.: Synthèse stratigraphique et paléogéographique sur les faciès urgoniens du Sud de l'Ardèche et du Nord du Gard (France SE). Geobios, 12, 121-139. https://doi.org/10.1016/S0016-6995(79)80055-8, 1979.

Dall'Asta, N., Hoareau, G., Manatschal, G., Centrella, S., Denèle, Y., Ribes, C., & Kalifi, A. : Structural and petrological characteristics of a Jurassic detachment fault from the Mont-Blanc massif (Col du Bonhomme area, France). Journal of Structural Geology, 159, 104593. https://doi.org/10.1016/j.jsg.2022.104593, 2022.

Dardeau, G., Atrops, F., Fortwengler, D., De Graciansky, P. C., & Marchand, D. : Jeux de blocs et tectonique distensive au Callovien et a l'Oxfordien dans le bassin du Sud-Est de la France. Bulletin de la Société géologique de France, 4(5), 771-777, 1988.

Debelmas, J. : La zone subbriançonnaise et la zone valaisanne savoyarde dans le cadre de la tectonique des plaques. Géologie Alpine, 77, 3-8, 1988, 2001.

Delvaux, D., & Sperner, B.: New aspects of tectonic stress inversion with reference to the TENSOR program. https://doi.org/10.1144/GSL.SP.2003.212.01.06, 2003.

Debrand-Passard, S. : Synthèse géologique du Sud-Est de la France (Vol. 1). Editions BRGM.de Graciansky, P.C., & Lemoine, Marcel., 1988. Early Cretaceous extensional tectonics in the xsouthwestern French Alps; a consequence of North-Atlantic rifting during Tethyan spreading. Bulletin de la Société géologique de France, 4(5), 733-737, 1984.

Dèzes, P., Schmid, S. M., & Ziegler, P. A. : Evolution of the European Cenozoic Rift System: interaction of the Alpine and Pyrenean orogens with their foreland lithosphere. Tectonophysics, 389(1-2), 1-33. https://doi.org/10.1016/j.tecto.2004.06.011, 2004.

Donard, A., Pottin, A. C., Pointurier, F., & Pécheyran, C.: Determination of relative rare earth element distributions in very small quantities of uranium ore concentrates using femtosecond UV laser ablation–SF-ICP-MS coupling. Journal of Analytical Atomic Spectrometry, 30(12), 2420-2428, 2015.

Espurt, N., Angrand, P., Teixell, A., Labaume, P., Ford, M., de Saint Blanquat, M., & Chevrot,

S. Crustal-scale balanced cross-section and restorations of the Central Pyrenean belt (Nestes-Cinca transect): Highlighting the structural control of Variscan belt and Permian-Mesozoic rift systems on mountain building. Tectonophysics, 764, 25-45. https://doi.org/10.1016/j.tecto.2019.04.026, 2019.

Flandrin, J. : Sur l'âge des principaux traits structuraux du Diois et des Baronnies. Bulletin de la Société géologique de France, 7(3), 376-386. https://doi.org/10.2113/gssgfbull.S7-VIII.3.376, 1966.

Ford, M., Lickorish, W.H. & Kusznir, N.J.: Tertiary foreland sedimentation in the southern Subalpine chains, SE France: a geodynamic analysis. Basin Research, 11, 315–336. https://doi.org/10.1046/j.1365-2117.1999.00103.x, 1999

Ford, M., & Lickorish, W. H.: Foreland basin evolution around the western Alpine Arc. https://doi.org/10.1144/GSL.SP.2004.221.01.04, 2004.

Ford, M., Masini, E., Vergés, J., Pik, R., Ternois, S., Léger, J., ... & Calassou, S.: Evolution of a low convergence collisional orogen: a review of Pyrenean orogenesis. BSGF-Earth Sciences Bulletin, 193(1), 19. https://doi.org/10.1051/bsgf/2022018, 2022.

Gidon, M., Arnaud, H., Pairis, J. L., AprAHAMIAN, J., & Uselle, J. P. : Les déformations tectoniques superposées du Dévoluy méridional (Hautes-Alpes). Géologie Alpine, 46, 87-110, 1970.

Girault, J. B., Bellahsen, N., Bernet, M., Pik, R., Loget, N., Lasseur, E., ... & Sonnet, M.: Exhumation of the Western Alpine collisional wedge: New thermochronological data. Tectonophysics, 822, 229155. https://doi.org/10.1016/j.tecto.2021.229155, 2022.

Guilhaumou, N., Touray, J. C., Perthuisot, V., & Roure, F., Palaeocirculation in the basin of southeastern France sub-alpine range: a synthesis from fluid inclusions studies. Marine and Petroleum Geology, 13(6), 695-706. https://doi.org/10.1016/0264-8172(95)00064-X. 1996.

Guyonnet-Benaize, C., Lamarche, J., Masse, J. P., Villeneuve, M., & Viseur, S. : 3D structural modelling of small-deformations in poly-phase faults pattern. Application to the Mid-Cretaceous Durance uplift, Provence (SE France). Journal of Geodynamics, 50(2), 81-93. https://doi.org/10.1016/j.jog.2010.03.003, 2010.

Hoareau, G., Claverie, F., Pecheyran, C., Barbotin, G., Perk, M., Beaudoin, N. E., ... & Rasbury, E. T.: The virtual spot approach: a simple method for image U-Pb carbonate geochronology by high-repetition rate LA-ICP-MS. EGUsphere, 2024, 1-35. https://doi.org/10.5194/egusphere-2024-2366, 2024.

Hoareau, G., Claverie, F., Pecheyran, C., Paroissin, C., Grignard, P. A., Motte, G., ... & Girard,

J. P.: Direct U–Pb dating of carbonates from micron-scale femtosecond laser ablation inductively coupled plasma mass spectrometry images using robust regression. Geochronology, 3(1), 67-87. https://doi.org/10.5194/ gchron-3-67-2021, 2021.

Homberg, C., Barrier, E., Mroueh, M., Muller, C., Hamdan, W., & Higazi, F.: Tectonic evolution of the central Levant domain (Lebanon) since Mesozoic time. https://doi.org/10.1144/SP341.12, 2010.

Homberg, C., Schnyder, J., & Benzaggagh, M.: Late Jurassic-Early Cretaceous faulting in the Southeastern French Basin: does it reflect a tectonic reorganization?. Bulletin de la Société géologique de France, 184(4-5), 501-514. https://doi.org/10.2113/gssgfbull.184.4-5.501, 2013.

Hippolyte, J. C., Angelier, J., Bergerat, F., Nury, D., & Guieu, G.: Tectonic-stratigraphic record of paleostress time changes in the Oligocene basins of the Provence, southern France. Tectonophysics, 226(1-4), 15-35. https://doi.org/10.1016/0040-1951(93)90108-V. 1993

Huang, Q., Geometry and tectonic significance of Albian sedimentary dykes in the Sisteron area, SE France, J. Struct. Geol., 10, 453–462, 1988.

Jolivet, L., Frizon de Lamotte, D., Mascle, A., & Séranne, M.: The Mediterranean basins: Tertiary extension within the Alpine orogen—An introduction. Geological Society, London, Special Publications, 156(1), 1-14. https://doi.org/10.1144/GSL.SP.1999.156.01.02, 1999

Jolivet, L., Menant, A., Roche, V., Le Pourhiet, L., Maillard, A., Augier, R., ... & Canva, A.: Transfer zones in Mediterranean back-arc regions and tear faults. Bulletin de la Société Géologique de France, 192(1). https://doi.org/10.1051/bsgf/2021006, 2021.

Joseph, P., Beaudoin, B., Sempere, T., & Maillart, J. : Vallées sous-marines et systèmes d'épandages carbonatés du Berriasien vocontien (Alpes méridionales françaises). Bull. Soc. Geol. Fr, 8, 363-374, 1988.

Kouketsu, Y., Mizukami, T., Mori, H., Endo, S., Aoya, M., Hara, H., ... & Wallis, S.: A new approach to develop the R aman carbonaceous material geothermometer for low-grade metamorphism using peak width. Island Arc, 23(1), 33-50. https://doi.org/10.1111/iar.12057, 2014.

Lacombe, O., Beaudoin, N. E., Hoareau, G., Labeur, A., Pecheyran, C., and Callot, J.-P.: Dating folding beyond folding, from layer-parallel shortening to fold tightening, using mesostructures: lessons from the Apennines, Pyrenees, and Rocky Mountains, Solid

Earth, 12, 2145–2157, https://doi.org/10.5194/se-12-2145-2021, 2021.Lacombe, O., Parlangeau, C., Beaudoin, N. E., & Amrouch, K. : Calcite twin formation,

measurement and use as stress strain indicators: a review of progress over the last decade. Geosciences, 11(11), 445. https://doi.org/10.3390/geosciences11110445, 2021.

Lahfid, A., Beyssac, O., Deville, E., Negro, F., Chopin, C., & Goffé, B. (2010). Evolution of the Raman spectrum of carbonaceous material in low-grade metasediments of the Glarus Alps (Switzerland). Terra nova, 22(5), 354-360. https://doi.org/10.1111/j.1365-3121.2010.00956.x, 2010.

Le Breton, E., Brune, S., Ustaszewski, K., Zahirovic, S., Seton, M., & Müller, R. D. : Kinematics and extent of the Piemont–Liguria Basin–implications for subduction processes in the Alps. Solid Earth, 12(4), 885-913. https://doi.org/10.5194/se-12-885-2021, 2021.

Lemoine, M. : Rythme et modalités des plissements superposés dans les chaînes subalpines méridionales des Alpes occidentales françaises. Geologische Rundschau, 61, 975-1010. https://doi.org/10.1007/BF01820902, 1972.

Lemoine, M., Bas, T., Arnaud-Vanneau, A., Arnaud, H., Dumont, T., Gidon, M., Bourbon, M., Graciansky, P.-C. de, Rudkiewicz, J.-L., Megard-Galli, J., and Tricart, P.: The continental margin of the Mesozoic Tethys in the Western Alps, Mar Petrol Geol, 3, 179–199, https://doi.org/10.1016/0264-8172(86)90044-9, 1986.Lemoine, M., Bas, T., Arnaud-Vanneau, A., Arnaud, H., Dumont, T., Gidon, M., ... & Tricart, P. (1986). The continental margin of the Mesozoic Tethys in the Western Alps. Marine and petroleum geology, 3(3), 179-199.

Lemoine, M., Tricart, P. and Boillot, G.: Ultramafic and gabbroic ocean floor of the

Ligurian Tethys (Alps, Corsica, Apennines): in search for a genetic model. Geology, 15: 622-625, 1987.

Manatschal, G., & Müntener, O.: A type sequence across an ancient magma-poor ocean–continent transition: the example of the western Alpine Tethys ophiolites. Tectonophysics, 473(1-2), 4-19. https://doi.org/10.1016/j.tecto.2008.07.021, 2009

Marchand, E., Séranne, M., Bruguier, O., & Vinches, M. : LA-ICP-MS dating of detrital zircon grains from the Cretaceous allochthonous bauxites of Languedoc (south of France): Provenance and geodynamic consequences. Basin Research, 33(1), 270-290. https://doi.org/10.1111/bre.12465, 2021.

Merle, O., & Michon, L.: The formation of the West European Rift; a new model as exemplified by the Massif Central area. Bulletin de la Societé géologique de France, 172(2), 213-221. https://doi.org/10.2113/172.2.213, 2021.

Mohn, G., Manatschal, G., Beltrando, M., & Haupert, I.: The role of rift-inherited hyper-extension in Alpine-type orogens. Terra Nova, 26(5), 347-353. https://doi.org/10.1111/ter.12104, 2014.

Montenat, C., Janin, M. C., & Barrier, P. : L'accident du Toulourenc: une limite Tectonique entre la plate-forme provençale et le Bassin vocontien à l'Aptien–Albien (SE France). Comptes rendus. Géoscience, 336(14), 1301-1310, 2004.

Mouthereau, F., Filleaudeau, P. Y., Vacherat, A., Pik, R., Lacombe, O., Fellin, M. G., ... & Masini, E.: Placing limits to shortening evolution in the Pyrenees: Role of margin architecture and implications for the Iberia/Europe convergence. Tectonics, 33(12), 2283-2314. https://doi.org/10.1002/2014TC003663, 2014.

Mouthereau, F., Angrand, P., Jourdon, A., Ternois, S., Fillon, C., Calassou, S., ... & Baudin, T.: Cenozoic mountain building and topographic evolution in Western Europe: impact of billions of years of lithosphere evolution and plate kinematics. BSGF-Earth Sciences Bulletin, 192(1), 56. https://doi.org/10.1051/bsgf/2021040, 2021.

Muñoz, J. A.: Evolution of a continental collision belt: ECORS-Pyrenees crustal balanced cross-section. In Thrust tectonics (pp. 235-246). Dordrecht: Springer Netherlands, 1992.

Olivetti, V., Godard, V., Bellier, O., & Aster Team.: Cenozoic rejuvenation events of Massif Central topography (France): Insights from cosmogenic denudation rates and river profiles. Earth and Planetary Science Letters, 444, 179-191. https://doi.org/10.1016/j.epsl.2016.03.049, 2016.

Parizot, O., Missenard, Y., Haurine, F., Blaise, T., Barbarand, J., Benedicto, A., & Sarda, P.: When did the Pyrenean shortening end? Insight from U–Pb geochronology of syn-faulting calcite (Corbières area, France). Terra nova, 33(6), 551-559. https://doi.org/10.1111/ter.12547, 2021.

Parizot, O., Missenard, Y., Barbarand, J., Blaise, T., Benedicto, A., Haurine, F., & Sarda, P.:

How sensitive are intraplate inherited structures? Insight from the Cévennes Fault System (Languedoc, SE France). Geological Magazine, 159(11-12), 2082-2094. https://doi.org/10.1017/S0016756822000152, 2022.

Ribes, C., Ghienne, J. F., Manatschal, G., Dall'Asta, N., Stockli, D. F., Galster, F., ... & Karner, G. D.: The Grès Singuliers of the Mont Blanc region (France and Switzerland): stratigraphic response to rifting and crustal necking in the Alpine Tethys. International Journal of Earth Sciences, 109, 2325-2352. https://doi.org/10.1007/s00531-020-01902-z, 2020.

Roure, F., Brun, J. P., Colletta, B., & Van Den Driessche, J.: Geometry and kinematics of extensional structures in the Alpine foreland basin of southeastern France. Journal of Structural Geology, 14(5), 503-519. https://doi.org/10.1016/0191-8141(92)90153-N, 1992.

Saspiturry, N., Lahfid, A., Baudin, T., Guillou-Frottier, L., Razin, P., Issautier, B., ... & Corre, B.: Paleogeothermal gradients across an inverted hyperextended rift system: Example of the Mauléon Fossil Rift (Western Pyrenees). Tectonics, 39(10), e2020TC006206. https://doi.org/10.1029/2020TC006206, 2020.

Schito, A., Romano, C., Corrado, S., Grigo, D., & Poe, B.: Diagenetic thermal evolution of organic matter by Raman spectroscopy. Organic Geochemistry, 106, 57-67. https://doi.org/10.1016/j.orggeochem.2016.12.006, 2017.

Schwartz, S., Gautheron, C., Audin, L., Dumont, T., Nomade, J., Barbarand, J., ... & van der Beek, P.: Foreland exhumation controlled by crustal thickening in the Western Alps. Geology, 45(2), 139-142, 2017

Schwartz, S., Rolland, Y., Nouibat, A., Boschetti, L., Bienveignant, D., Dumont, T., ... & Mouthereau, F.: Role of mantle indentation in collisional deformation evidenced by deep geophysical imaging of Western Alps. Communications Earth & Environment, 5(1), 17. https://doi.org/10.1038/s43247-023-01180-y, 2024.

Séranne, M.: The Gulf of Lion continental margin (NW Mediterranean) revisited by IBS: an overview. Geological Society, London, Special Publications, 156(1), 15-36. https://doi.org/10.1144/GSL.SP.1999.156.01.03, 1999.

Séranne, M., Couëffé, R., Husson, E., Baral, C., & Villard, J. : The transition from Pyrenean shortening to Gulf of Lion rifting in Languedoc (South France)–A tectonic-sedimentation analysis. BSGF-Earth Sciences Bulletin, 192(1), 27, 2021.

Simon-Labric, T., Rolland, Y., Dumont, T., Heymes, T., Authemayou, C., Corsini, M., and Fornari, M.: 40Ar/39Ar dating of Penninic Front tectonic displacement (W Alps) during the Lower Oligocene (31–34 Ma), Terra Nova, 21, 127–136, https://doi.org/10.1111/j.1365-3121.2009.00865.x, 2009.

Simon-Labric, T., Rolland, Y., Dumont, T., Heymes, T., Authemayou, C., Corsini, M., & Fornari, M. (2009). 40Ar/39Ar dating of Penninic Front tectonic displacement (W Alps) during the Lower Oligocene (31–34 Ma). *Terra Nova*, *21*(2), 127-136.Teixell, A., Labaume, P., Ayarza, P., Espurt, N., de Saint Blanquat, M., & Lagabrielle, Y.: Crustal structure and evolution of the Pyrenean-Cantabrian belt: A review and new interpretations from recent concepts and data. Tectonophysics, 724, 146-170. https://doi.org/10.1016/j.tecto.2018.01.009, 2018.

Tigroudja, L., Espurt, N., & Scalabrino, B.: Quantifying Miocene thin-and thick-skinned shortening in the Baous thrust system, SW French Alpine Front. Tectonophysics, 230930, 2025.

Trümpy, R.: A possible Jurassic-Cretaceous transform system in the Alps and the Carpathians. https://doi.org/10.1130/SPE218-p93, 1988.

Turco, E., Macchiavelli, C., Mazzoli, S., Schettino, A., & Pierantoni, P. P. : Kinematic evolution of Alpine Corsica in the framework of Mediterranean mountain belts. Tectonophysics, 579, 193-206, 2012.

Vacherat, A., Mouthereau, F., Pik, R., Bellahsen, N., Gautheron, C., Bernet, M., Daudet, M., Balansa, J., Tibari, B., Jamme, R. P., and Radal, J.: Rift-to-collision transition recorded by tectonothermal evolution of the northern Pyrenees, Tectonics, 35, 907–933, https://doi.org/10.1002/2015tc004016, 2016.

Wicker, V., & Ford, M.: Assessment of the tectonic role of the Triassic evaporites in the North Toulon fold-thrust belt. BSGF-Earth Sciences Bulletin, 192(1), 51. https://doi.org/10.1051/bsgf/2021033, 2021.

Zeboudj, A., Lacombe, O., Beaudoin, N. E., Callot, J. P., Lamarche, J., Guihou, A., & Hoareau, G.: Sequence, duration, rate of deformation and paleostress evolution during fold development: Insights from fractures, calcite twins and U-Pb calcite geochronology in the Mirabeau anticline (SE France). Journal of Structural Geology, 105460. https://doi.org/10.1016/j.jsg.2025.105460, 2025.

Ziegler, P. A., & Dèzes, P.: Crustal evolution of western and central Europe. https://doi.org/10.1144/GSL.MEM.2006.032.01.03, 2006.

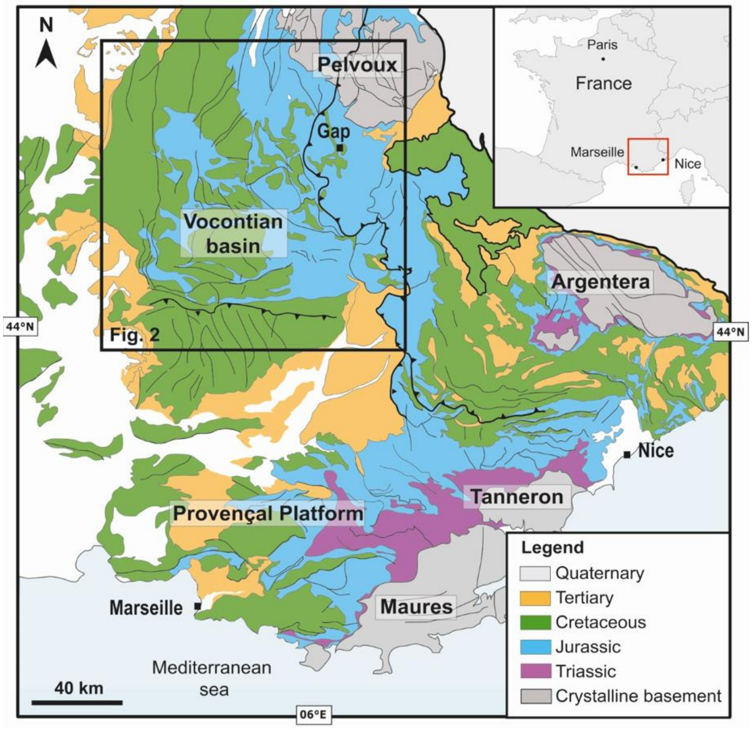

Figure 1: Simplified geological map of SE France. Location of the study area.

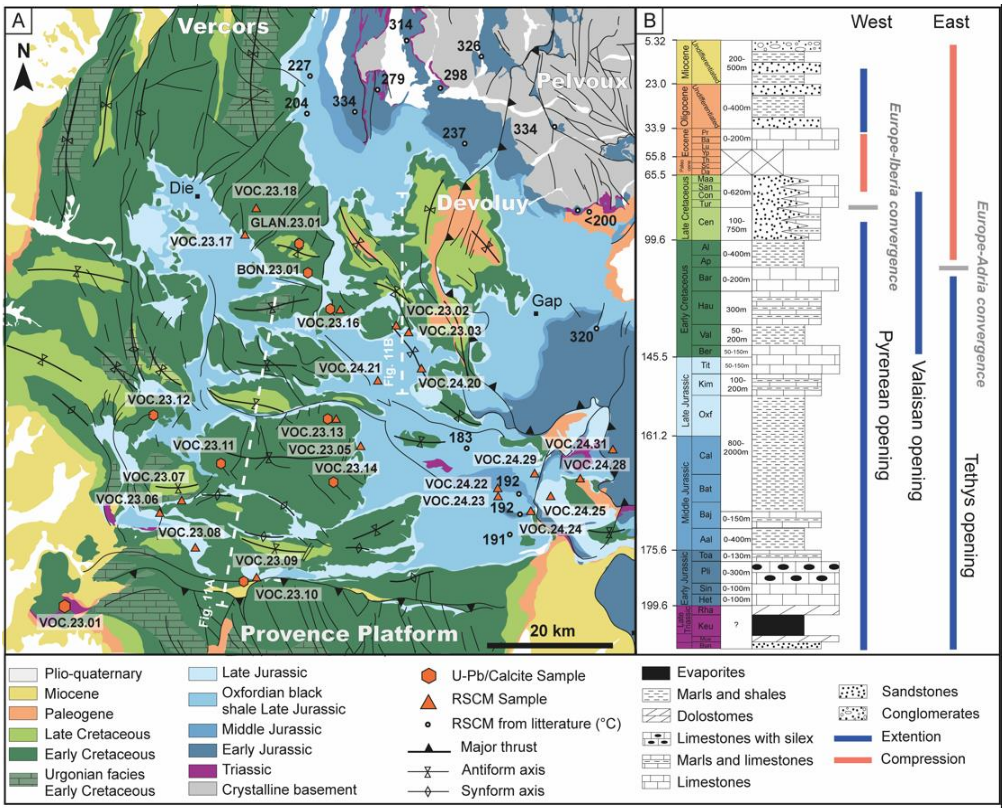

Figure 2: A) Geological map of Vocontian basin with sample location and Raman data in °C from Bellanger et al. (2015) and Célini et l. (2023). B) General stratigraphic section of the Vocontian basin and main tectonic events.

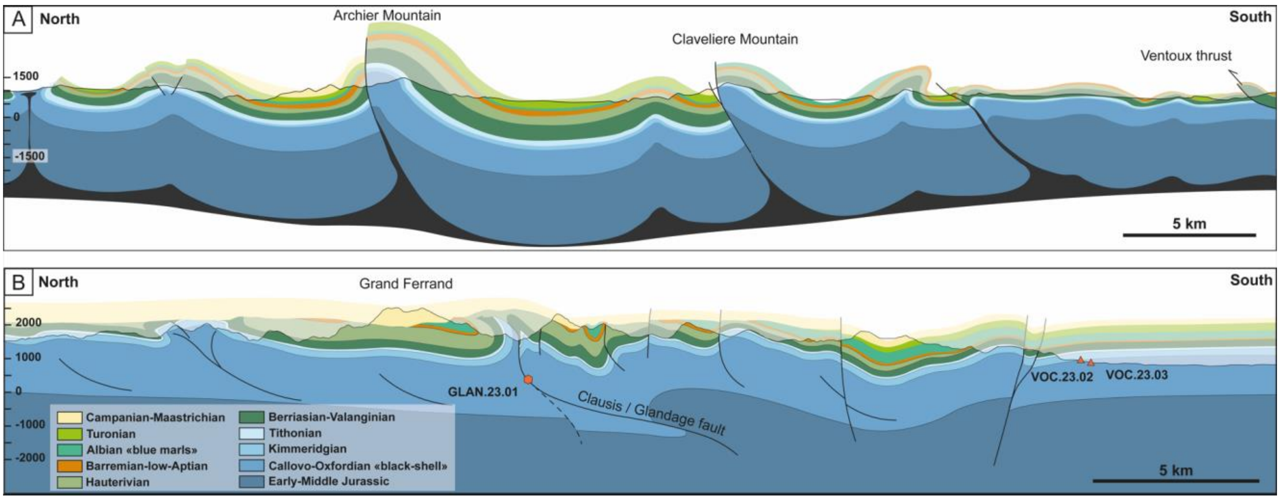

Figure 3: North-South geological cross-section of the Vocontian basin (A) and the Dévoluy massif (B). Location is presented in Fig. 2. Coniacian and Santonian are missing as there is a sedimentary gap (see in the text).

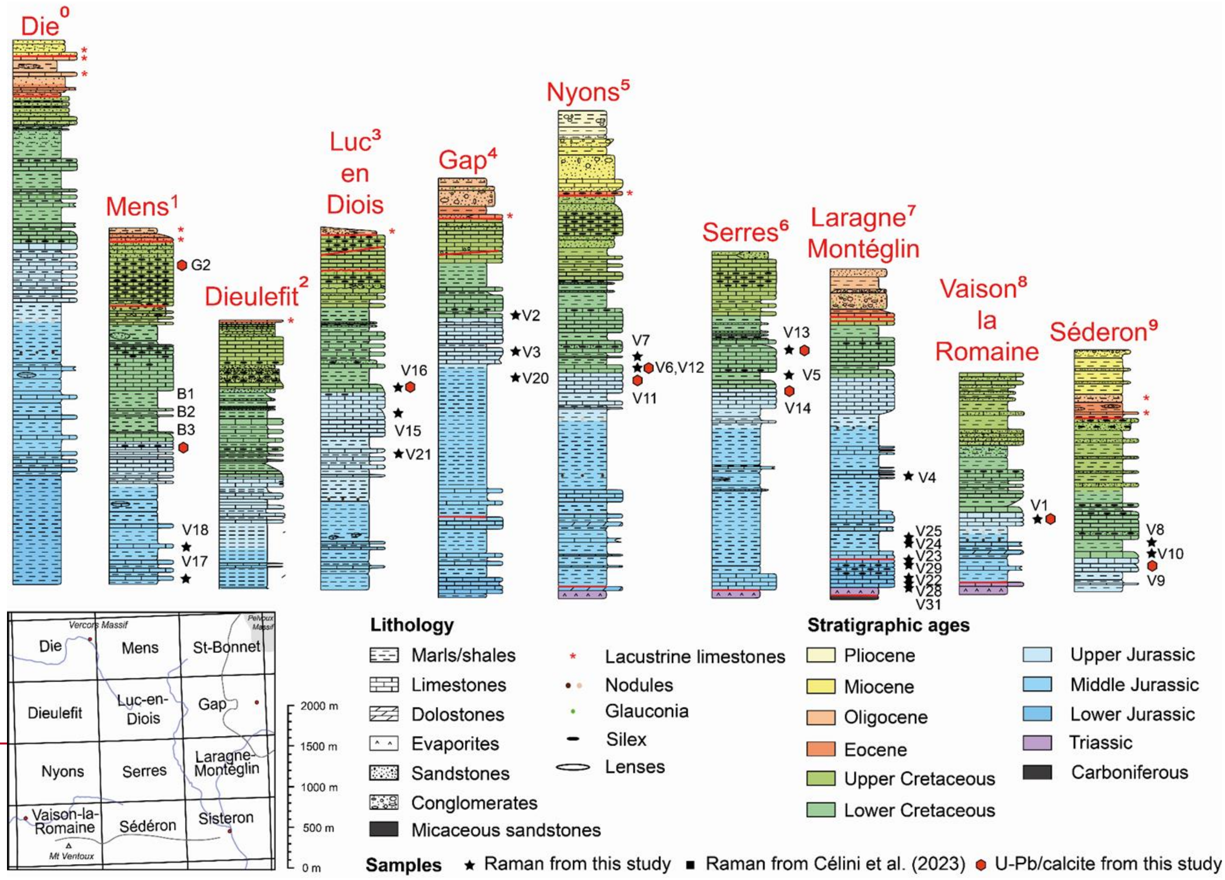

Figure 4: Stratigraphic logs corresponding to each geological notice of BRGM maps from the Vocontian basin. Sample names are shortened from V.23.X to VX for simplification and space in the figure.

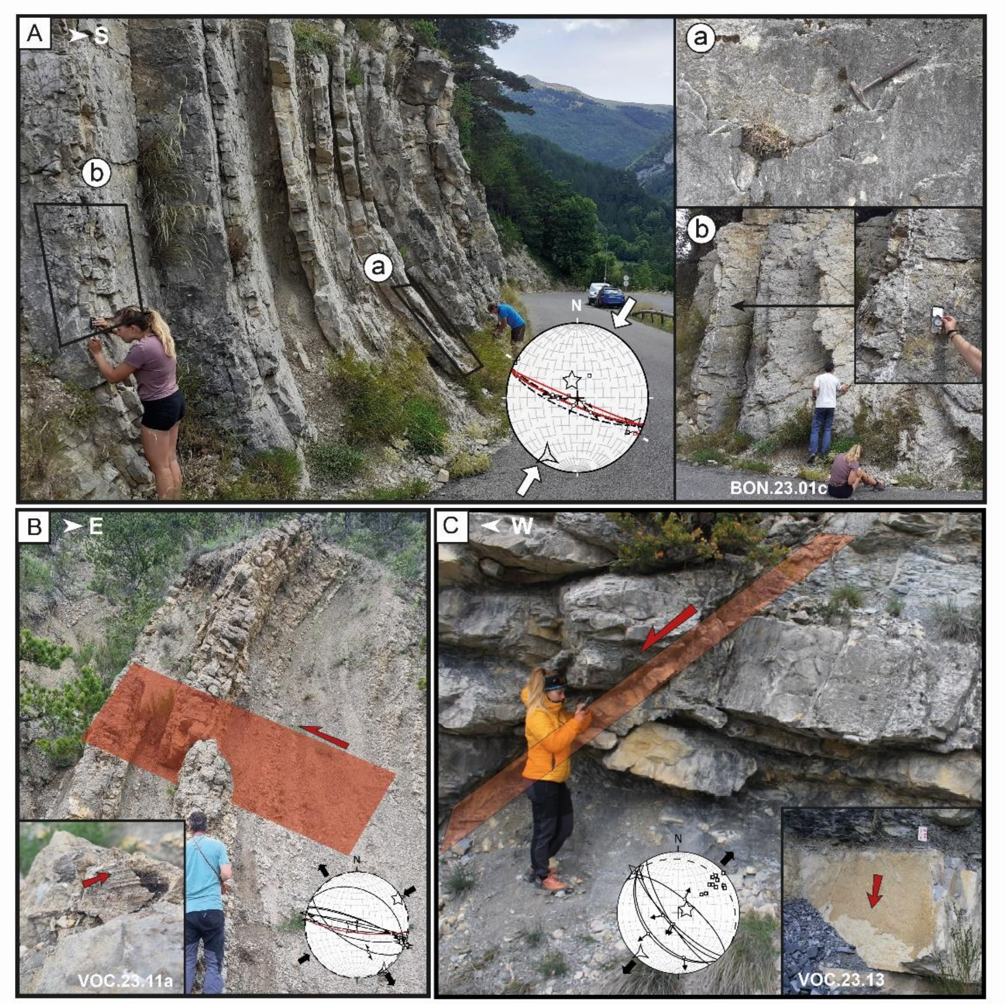

Figure 5: Main geological structures associated to their corresponding measurement and U-Pb age. A) sample BON.23.01. B) sample VOC.23.11. C) sample VOC.23.13.

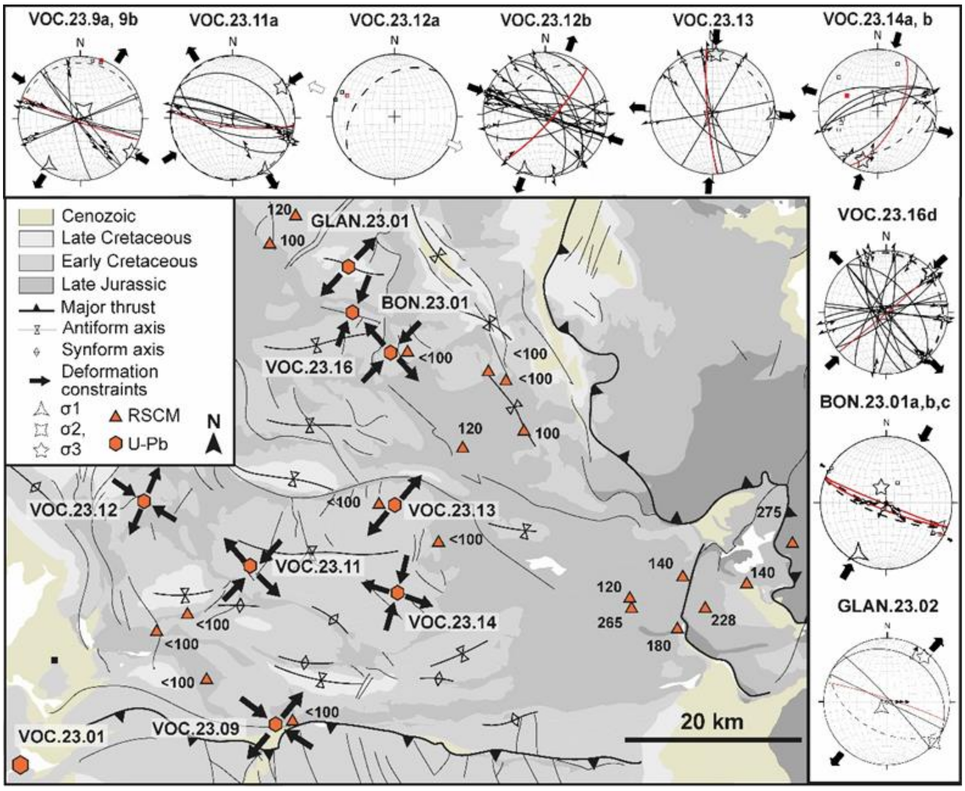

Figure 6: Simplified geological map with structural analysis of each dated sample and location of Raman thermometry results given in °C.

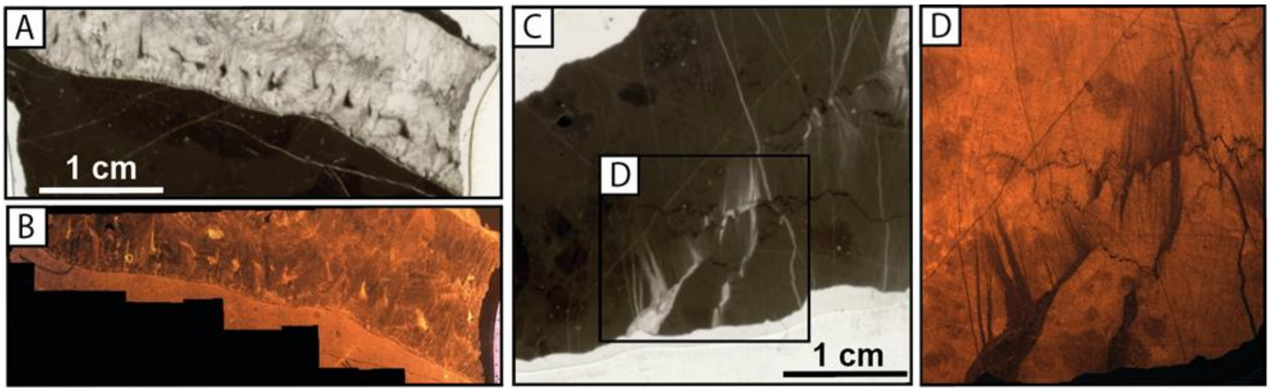

Figure 7: Examples of LPNA (A and C) and cathodolumiscence microphotographs (B and D) of two different types of U/Pb-dated calcite veins. A) and B) sample VOC-23-01. C) and D) sample VOC-23-11a.

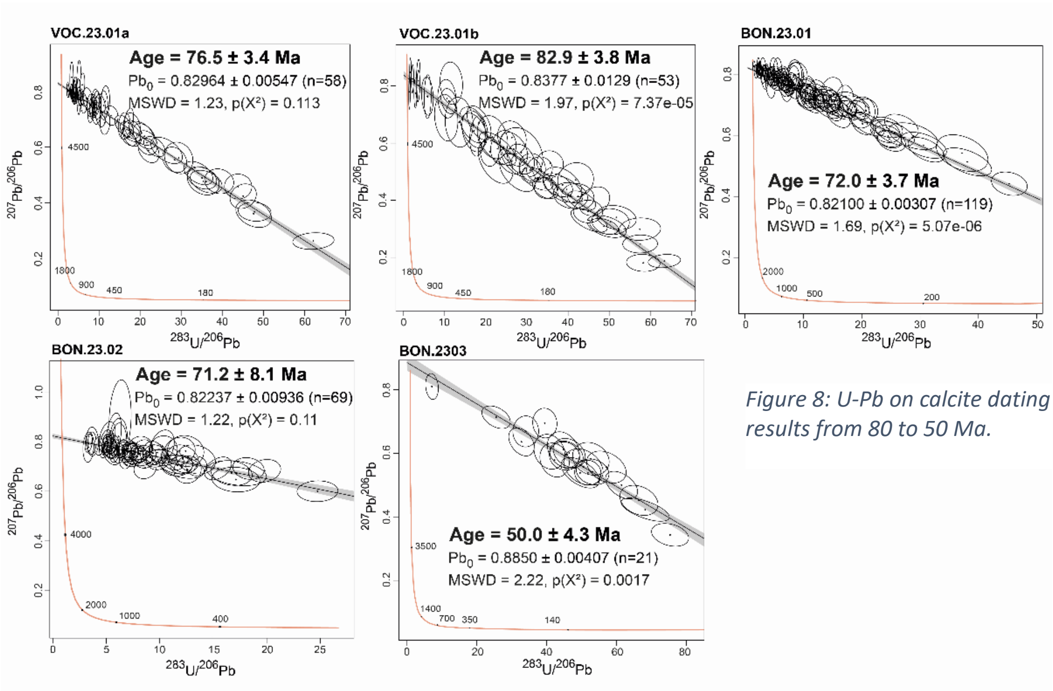

Figure 8: U-Pb on calcite dating results from 80 to 50 Ma.

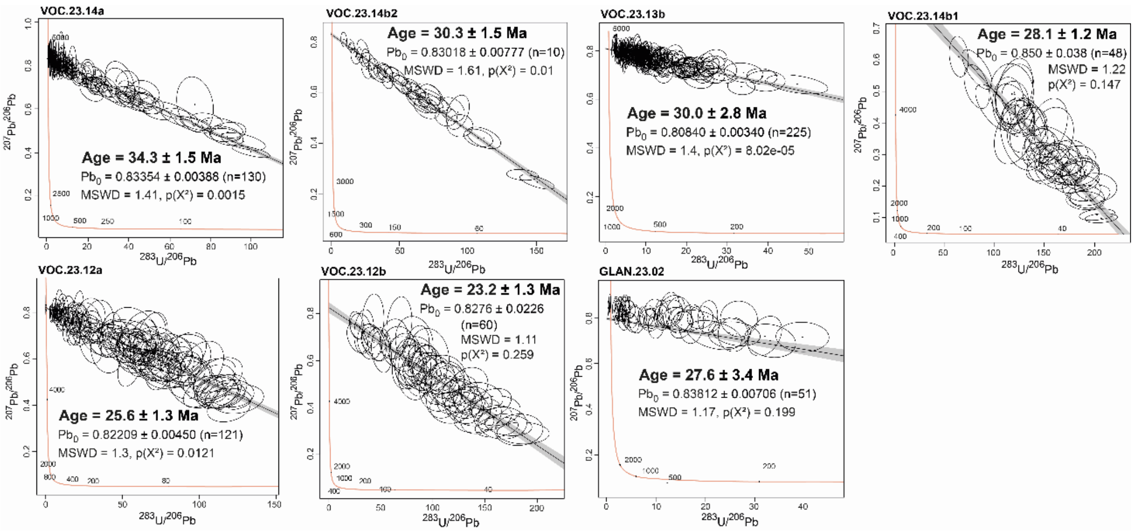

Figure 9: U-Pb on calcite dating results from 30 to 20 Ma.

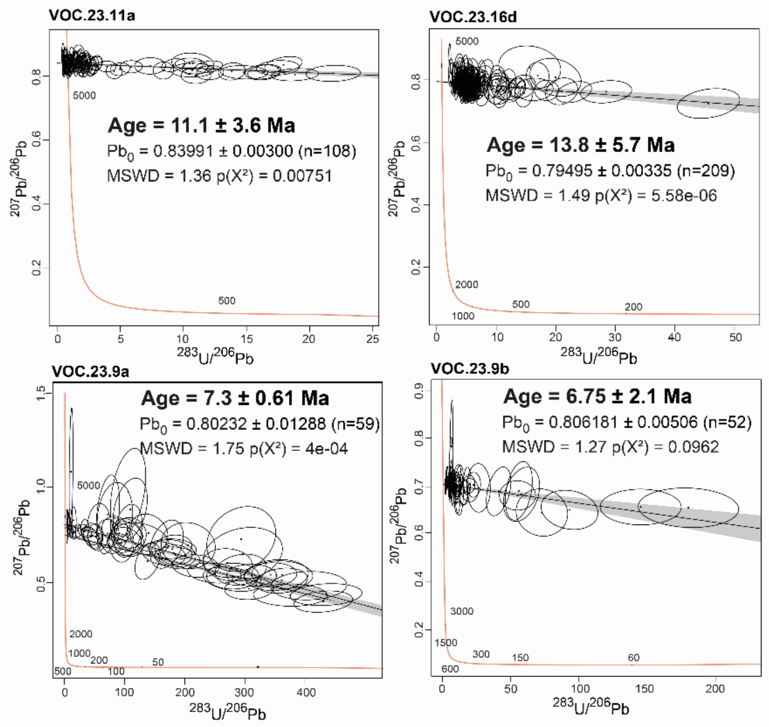

Figure 10: U-Pb on calcite dating results from 12 to 7 Ma.

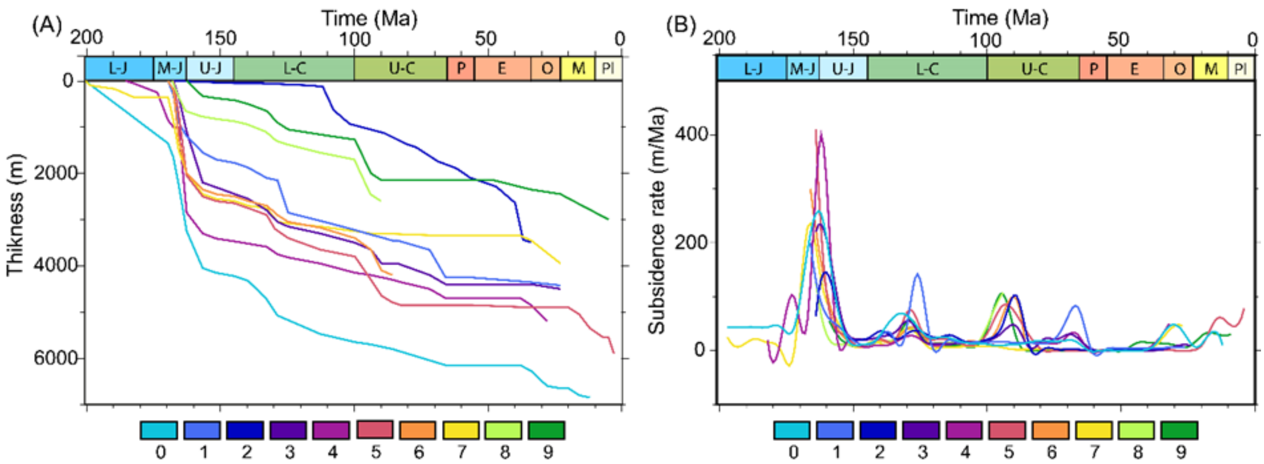

Figure 11: A) Burial history computed after the synthetic stratigraphic sections shown in Figure 10. B) evolution of sediment accumulation rate through time. 0: Die; 1: Dieulefit; 2: Gap; 3: Laragne-Montéglin; 4: Luc-en-Diois; 5: Mens; 6: Nyons; 7: Sédéron; 8: Serre; 9: Vaison-la-Romaine. L: lower, mi: middle; u: upper; J: jurassic; C: cretaceous; p: Paleocene; e: Eocene; o: Oligocene; m: Miocene; pl: Pliocene.

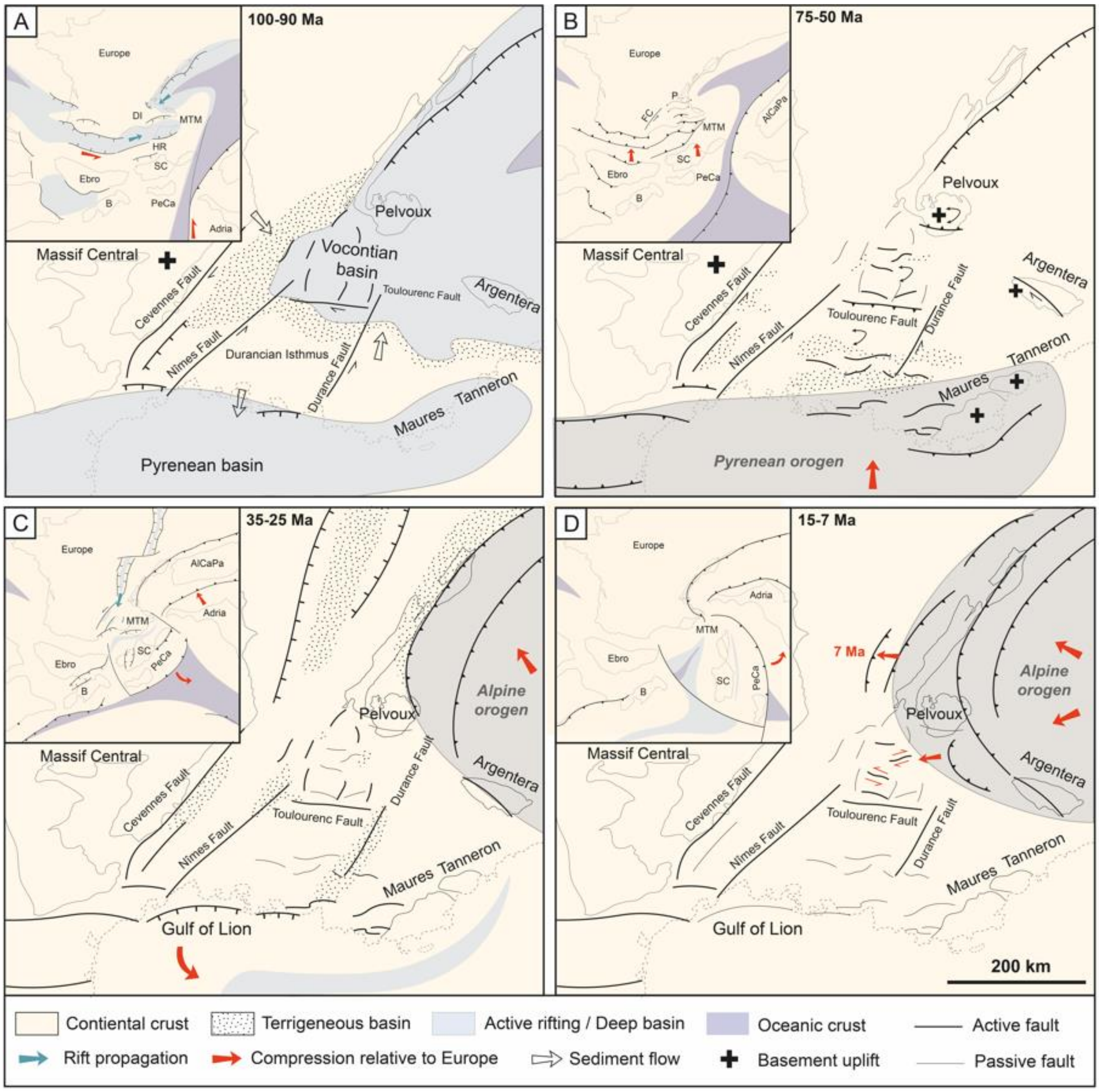

Figure 12: Regional tectonic and paleogeographical reconstitutions of SE France showing the evolution of the Vocontian basin since the Middle Cretaceous (modified after Boschetti et al., 2025b). A) Rifting in overlapping Pyrenean-Vocontian rift segments at 110-90 Ma. B) Pyrenees-Provence collision phase from 75 to 50 Ma. C) Opening of the West European Rift and onset of Alpine foreland fold and thrust belt tectonics. D) Alpine collision and westward propagation of deformation front. SC: Corsica-Sardinia; B: Baleares; C: Chartreuse; V: Vercors.

Table 1: Calcite sample types and correspondinng measurements and ages.

Sample	Lat	Long	Structures	n	σ1	σ2	σ3	ϕ	U-Pb (Ma)	Error (Ma)
VOC.23.01a	44.159326	5.049163	Vein + Strike slip	-	-	-	-	-	76.5	3.4
VOC.23.02b	44.159326	5.049163	Vein	-	-	-	-	-	82.9	3.8
VOC.23.9a	44.190622	5.47628	Strike-slip (Reverse)	13	02/124	80/025	10/214	0.6	7.3	0.61
VOC.23.9b	44.190622	5.47628	Vein (Associated 9a)	11	73/098	16/291	04/200	0.5	6.75	2.1
VOC.23.11a	44.367914	5.352686	Strike-slip (Post-fold)	6	17/0.23	71/185	05/292	0.5	11.1	3.6
VOC.23.12a	44.437467	5.293520	Vein	-	-	-	-	-	25.6	1.3
VOC.23.12b	44.437467	5.293520	Vein + Strike slip	17	10/292	78/078	06/201	0.5	23.2	1.3
VOC.23.13b	44.417889	5.657694	Normal fault	14	78/069	05/315	10/223	0.5	30	2.8
VOC.23.14a	44.328944	5.631972	Vein (Associated 14b)	-	-	-	-	-	34.3	1.5
VOC.23.14b1	44.328944	5.631972	Strike-slip (Normal)	6	17/197	73/007	03/106	0.5	30.3	1.5
VOC.23.14b2	44.328944	5.631972	Strike-slip (Normal)	6	17/197	73/007	03/106	0.5	28.1	1.2
VOC.23.16d	44.575833	5.640667	Strike-slip (Reverse)	20	04/048	86/234	00/138	0.5	13.8	5.7
BON.23.01a	44.62582	5.60985	Plane from fold	11	36/205	04/112	54/017	0.27	72	3.7
BON.23.01	44.62582	5.60985	Plane from fold	11	36/205	04/112	54/017	0.27	71.2	8.1
BON.23.01	44.62582	5.60985	Vein	11	36/205	04/112	54/017	0.27	50	4.3
GLAN.23.02	44.68617	5.59384	Normal fault	4	62/203	04/300	27/032	0.5	27.6	3.4

Table 2: Raman Thermometry data.

Sample	Lat °N	Lon °E	Stratigraphic Age (Ma)	Log/Map	Burial T (30°C/km)	Burial T (60°C/km)	RSCM T (°C)	1s
VOC.23.02	44.556889	5.772778	142	Gap	52	104	<100	
VOC.23.03	44.546834	5.801242	156	Gap	57	114	<100	
VOC.23.05	44.354736	5.668139	135	Serres	51	102	<100	
VOC.23.06	44.296138	5.281886	142	Nyons	51	102	<100	
VOC.23.07	44.299667	5.312604	142	Nyons	51	102	<100	
VOC.23.08	44.227526	5.433728	137	Sederon	75	150	<100	
VOC.23.10	44.221778	5.429244	142	Sederon	77.5	155	<100	
VOC.23.13	44.417889	5.657694	124	Serres	34.5	69	<100	
VOC.23.16	44.575833	5.640667	142	Luc-en-Diois	61.5	123	<100	
VOC.24.17	44.681803	5.414283	167	Mens	122	245	100	20
VOC.24.18	44.698656	5.419786	166	Mens	105	211	120	20
VOC.24.20	44.502694	5.820133	156	Gap	57	114	100	20
VOC.24.21	44.464336	5.697017	157	Luc-en-Diois	69	138	120	20
VOC.24.22	44.316244	5.959372	169	Laragne-Monteglin	93	186	120	20
VOC.24.23	44.308639	5.956206	166	Laragne-Monteglin	73	147	265	12
VOC.24.24a	44.281517	6.014347	163	Laragne-Monteglin	58.5	117	180	20
VOC.24.25	44.294617	6.056911	162	Laragne-Monteglin	58.5	117	228	22
VOCY.24.28a	44.328152	6.128097	170	Laragne-Monteglin	108	216	140	20
VOC.24.29	44.335796	6.020728	166	Laragne-Monteglin	73	147	140	20
VOC.24.31	44.357159	6.166843	175	Laragne-Monteglin	>108	>216	275	6